JOURNAL OF GEOPHYSICAL RESEARCH, VOL. 111, D12307, doi:10.1029/2005JD006072, 2006

A 12,000 year record of explosive volcanism in the Siple Dome Ice Core, West Antarctica

A. V. Kurbatov,[1] G. A. Zielinski,[1] N. W. Dunbar,[2] P. A. Mayewski,[1] E. A. Meyerson,[1] S. B. Sneed,[1] and K. C. Taylor[3]

Received 13 April 2005; revised 7 February 2006; accepted 27 February 2006; published 22 June 2006.

[1] Air mass trajectories in the Southern Hemisphere provide a mechanism for transport to and deposition of volcanic products on the Antarctic ice sheet from local volcanoes and from tropical and subtropical volcanic centers. This study extends the detailed record of Antarctic, South American, and equatorial volcanism over the last 12,000 years using continuous glaciochemical series developed from the Siple Dome A (SDMA) ice core, West Antarctica. The largest volcanic sulfate spike (280 μg/L) occurs at 5881 B.C.E. Other large signals with unknown sources are observed around 325 B.C.E. (270 μg/L) and 2818 B.C.E. (191 μg/L). Ages of several large equatorial or Southern Hemisphere volcanic eruptions are synchronous with many sulfate peaks detected in the SDMA volcanic ice chemistry record. The microprobe "fingerprinting" of glass shards in the SDMA core points to the following Antarctic volcanic centers as sources of tephra found in the SDMA core: Balenny Island, Pleiades, Mount Berlin, Mount Takahe, and Mount Melbourne as well as Mount Hudson and possibly Mount Burney volcanoes of South America. Identified volcanic sources provide an insight into the poorly resolved transport history of volcanic products from source volcanoes to the West Antarctic ice sheet.

Citation: Kurbatov, A. V., G. A. Zielinski, N. W. Dunbar, P. A. Mayewski, E. A. Meyerson, S. B. Sneed, and K. C. Taylor (2006), A 12,000 year record of explosive volcanism in the Siple Dome Ice Core, West Antarctica, *J. Geophys. Res.*, *111*, D12307, doi:10.1029/2005JD006072.

1. Introduction

[2] As has been documented previously [e.g., *Hammer et al.*, 1980; *Robock and Free*, 1995; *Zielinski*, 2000; *Mosley-Thompson et al.*, 2003], volcanic records recovered from ice cores drilled from the polar regions provide the best means to evaluate the impact of volcanism on global climate [*Robock*, 2000]. Continuous long-term records of SO_4^{2-} concentrations [*Mayewski et al.*, 1986, 1997; *Legrand et al.*, 1988; *Mosley-Thompson et al.*, 1991; *Delmas et al.*, 1992; *Zielinski et al.*, 1994, 1996b; *Langway et al.*, 1995; *Cole-Dai et al.*, 1997; *Jouzel et al.*, 2001; *Stenni et al.*, 2002; *Castellano et al.*, 2004, 2005], total acidity records from electrical conductivity (ECM) [*Hammer et al.*, 1980; *Hammer*, 1983; *Taylor et al.*, 1993; *Taylor and Alley*, 2004; *Wolff et al.*, 1995; *Clausen et al.*, 1997; *Karlöf et al.*, 2000], and dielectric profiling (DEP) [*Moore et al.*, 1989; *Udisti et al.*, 2000] methods detect the presence of volcanically produced aerosols and can be used to estimate the atmospheric loading of H_2SO_4, the primary climate-forcing component of an eruption [*Self et al.*, 1981; *Rampino and Self*, 1982, 1984; *Zielinski*, 1995]. These same records improve the overall chronological record of global volcanism [e.g., *Simkin and Siebert*, 1994]. Furthermore, these robust records provide a means to evaluate the volcano-climate system under different climatic modes than presently exists, and they provide critical information on how the type or frequency of eruptions may impact climatic conditions. The climatic impact of both multiple eruptions closely spaced in time and megaeruptions (e.g., Toba eruption of approximately 75,000 years ago [*Ninkovich et al.*, 1978; *Rose and Chesner*, 1987; *Zielinski et al.*, 1996a; *Oppenheimer*, 2002]) also may be different. However, deficiencies remain in the information currently available from existing ice core records of volcanism and the continued collection of highly resolved lengthy records from both Greenland and Antarctica remains a high priority for attaining a complete understanding of the volcanism-climate system. Spatial variability in the timing and magnitude of volcanic signals among cores also dictates that additional ice cores be evaluated, thereby increasing the confidence in estimates of atmospheric loading from past volcanic eruptions. The volcanic record that we present from the Siple Dome A ice core (hereafter SDMA), West Antarctica (Figure 1) is a contribution to solving some of these problems.

[3] Deficiencies in the ice core volcanic records available from the two polar regions are a function of several factors. One key factor is the temporal nature of the existing ice core derived volcanic record from Antarctica. Available annually

[1]Climate Change Institute, University of Maine, Orono, Maine, USA.
[2]New Mexico Bureau of Geology and Mineral Resources and Department of Earth and Environmental Science, New Mexico Institute of Mining and Technology, Socorro, New Mexico, USA.
[3]Desert Research Institute, University of Nevada, Reno, Nevada, USA.

0148-0227/06/2005JD006072$09.00

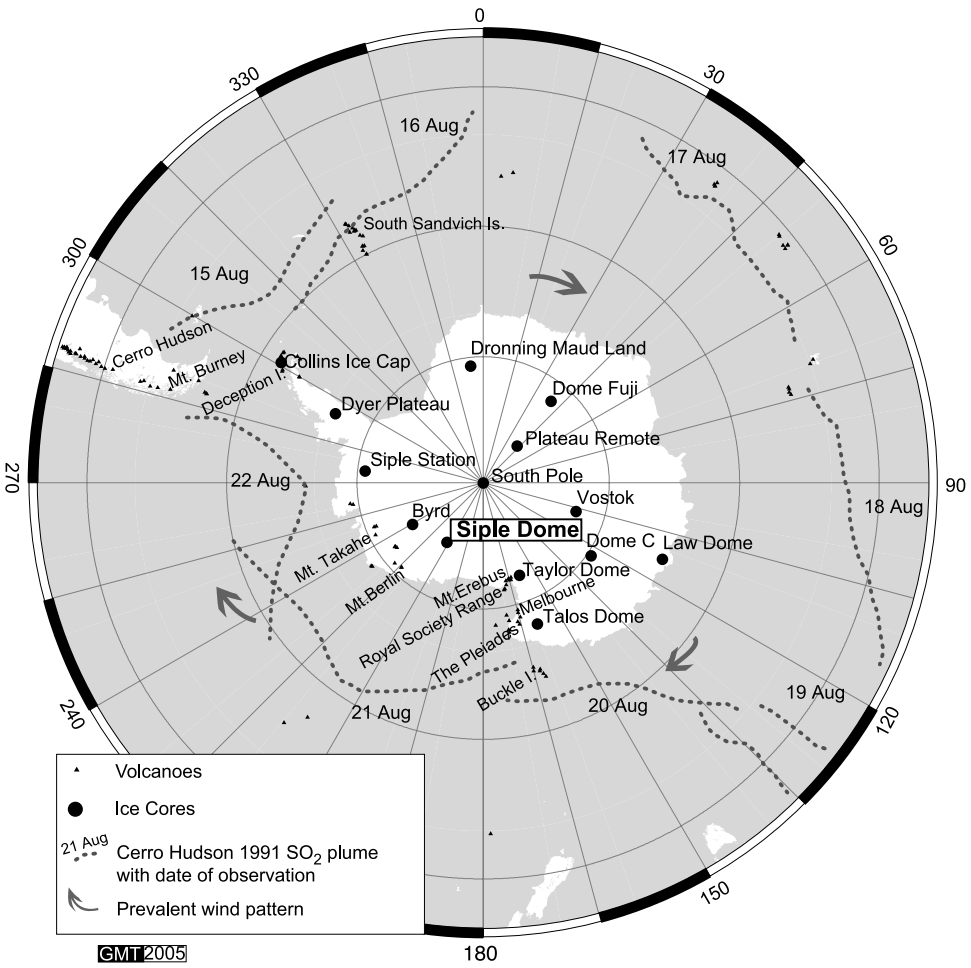

Figure 1. Location of Antarctic ice cores, volcanic centers, and prevalent wind pattern over Antarctica. Composite path of Cerro Hudson 1991 SO_2 plume is based on images taken by HIRS/2 platform [*Prata et al.*, 2003].

dated records from Antarctica (Figure 2) only extend back to 1300 C.E. at Law Dome ice core, East Antarctica [*Palmer et al.*, 2001], to 1443 C.E. at Siple Station, to 1417 C.E. at Dyer Plateau drill sites [*Cole-Dai et al.*, 1997], and to 1113 C.E. at South Pole [*Budner and Cole-Dai*, 2003]. Although the length of some ice core records from Antarctica may be high (e.g., the 420,000 years covered in the Vostok record [*Petit et al.*, 1999] or the recently recovered 740,000 years long record reported by *EPICA Community Members* [2004]) the overall lower accumulation found across most of Antarctica compared to that for Greenland limits the temporal resolution of the volcanic records produced from Antarctica. SDMA is annually dated to 8,600 years before 1950 C.E. (corresponding depth for this age is 514 m) providing the resolution needed to develop an excellent volcanic record for most of the Holocene via the SDMA SO_4^{2-} time series. Visible annual layers were observed in the SDMA ice core to a depth of 646 m (R.B. Alley, unpublished data at http://waiscores.dri.edu) which corresponds to the 12,000 yearlong interval [*Taylor et al.*, 2004] covered in this report.

[4] Another aspect of the volcanic record developed from Antarctic ice cores that needs improvement is differentiating among similar depositional fluxes (similar measured sulfate magnitudes) derived from equatorial eruptions, from Southern Hemisphere midlatitude eruptions, and from local (Antarctic Plate) eruptions. In the Northern Hemisphere the chronology of volcanism from Iceland is reasonably well established and signals from small Icelandic eruptions that probably have little climatic impact can be identified in Greenland ice cores and separated from the more climatically significant equatorial or other midlatitude eruptions [*Langway et al.*, 1995; *Zielinski*, 1995; *Zielinski et al.*, 1995; *Clausen et al.*, 1997; *Mosley-Thompson et al.*, 2003]. However, this scenario does not hold true for Antarctica. The chronology of Antarctic volcanism is poorly constrained given the remoteness of the continent. Consequently, identifying an Antarctic source for a particular signal may be problematic. For instance, have signals found in Antarctic ice cores that cannot be linked to equatorial or midlatitude eruptions originated from a previously unknown eruption in those parts of the globe or are these signals from Antarctic (i.e., local) eruptions? Our work attempts to answer this question.

[5] Tephra particles from several volcanic eruptions of Central and South America were previously found in the South Pole ice core [*Palais et al.*, 1990, 1992] which demonstrates, as expected, that volcanic products from

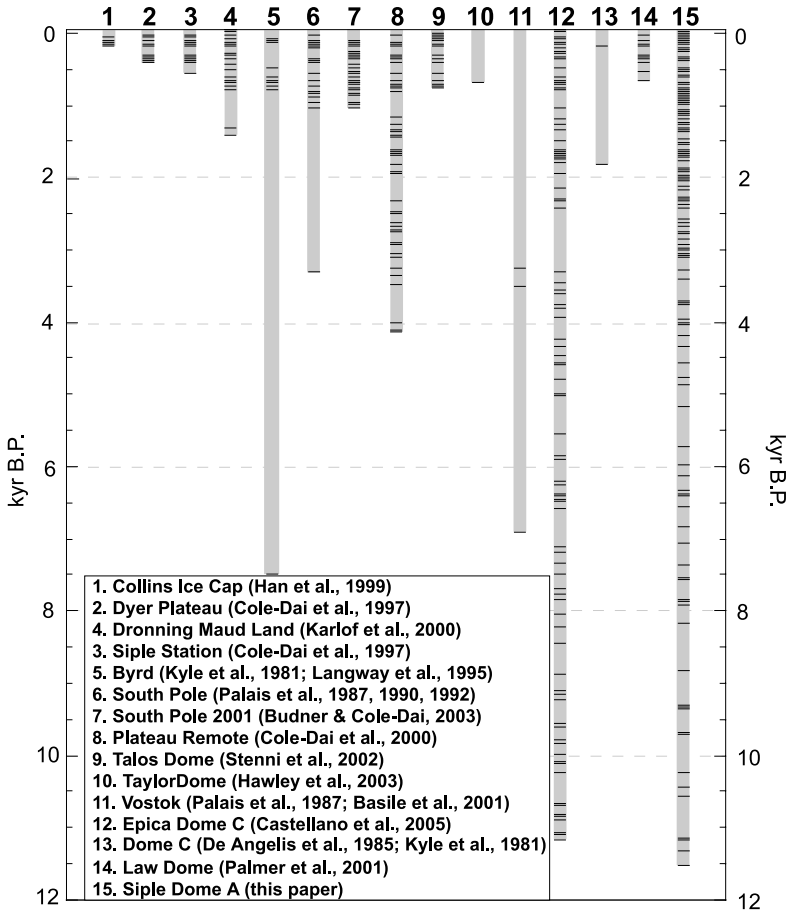

Figure 2. Length of previously developed Holocene volcanic records from Antarctica compared to that for the SDMA ice core in this study. In each record, volcanic signals determined by different methods are shown by black lines.

tropical and Southern Hemisphere volcanoes are transported to the Antarctic continent. The path of a volcanic plume from the August 15, 1991 Cerro Hudson volcanic eruption monitored by the HIRS/2 instrument (Figure 1) certainly confirms that a volcanic cloud injected into the upper troposphere to lower stratosphere could encircle the hemisphere within 9 days [*Prata et al.*, 2003]. Ice core and remote sensing data, as well as evidence of Patagonian origin dust found in Antarctica [*Basile et al.*, 1997], supports the existence of possible tropospheric pathways between the South American continent and Antarctica. Because of such atmospheric circulation patterns around Antarctica, tephra and sulfate aerosols are likely to be transported to the SDMA site from source volcanoes in South America.

[6] We developed the tephrochronology of the SDMA ice core as a means of improving the chronology of Antarctic volcanism for the Holocene as well as for improving the chronology of non-Antarctic eruptions. Ice core tephrochronology is undertaken by locating microscopic glass shards dispersed in layers of ice and by determining the chemical composition of that glass using an electron microprobe [*De Angelis et al.*, 1985]. The composition of these tiny particles is then matched to that of a known volcanic eruption or to the composition of material originating from known volcanic centers located in a region that is likely to deposit material at the ice core site. This procedure is similar to one that was done previously for visible ash layers found in Icelandic glaciers [*Thorarinsson*, 1944; *Self and Sparks*, 1981]. A successful match verifies the source volcano and timing of the related eruption consequently refining source eruptions responsible for the volcanochemical signals. Because of the proximity of the SDMA ice core to Antarctic volcanic centers it is expected that signals from local volcanism are especially prevalent in the SDMA record. Therefore our record will greatly augment volcanic records produced from other parts of Antarctica (Figure 2).

2. Methods

2.1. Core Location, Dating, and Sampling Methods

[7] The SDMA ice core (Figure 1) at 81°39.53′S, 148°48.72′W, 621 m was drilled to bedrock during the 1996–1998 austral summers as part of the WAISCORES scientific program. *Hamilton* [2002] reports 42 year average accumulation rates at 7 sites in the range of 0.086–0.155 m per year in water equivalent. The long-term accumulation rates can be significantly different from these measurements. The evidence from Vostok and Dome C ice cores [*Ciais et al.*, 1994; *Petit et al.*, 1999] show that 100% increase in snow accumulation rate is possible. The total ice depth of 1004 meters insured recovery of about a 97.5 kyr

old environmental record [*Brook et al.*, 2005]. We present only the record from the Holocene part of the core because the timescale for the 12,000 yearlong portion is developed by counting seasonal layers with several methane and tephra-based age control points [*Taylor et al.*, 2004].

[8] Ice handling and sampling procedures similar to those outlined by *Mayewski et al.* [1987] were used to insure lack of possible contamination, good sample quality, and repeatability of analyses. The inner, clean, sample melted from the 3.4 × 2.4 cm section of the ice core down to the depth of 624 m was analyzed using Dionex DX-500 ion chromatographs yielding 2817 discrete samples for ppb (μg/L) concentrations of major ions Cl^-, SO_4^{2-}, NO_3^-, K^+, Ca^{2+}, Na^+, Mg^{2+}. The sampling intervals of ~20 cm represents approximately a resolution 2.5 years per sample at the top of the core and about 4.9 years at 624 m depth.

[9] For the tephra studies, 1963 discrete samples were cut to the depth of 213.5 m from a 2.4 × 0.9 cm section of core. The length of these approximately annual samples varied from about 40 cm at the top to 5 cm at the end of the upper two millennia interval of the SDMA core. The remaining 2159 tephra samples from the interval 213.5–624 m were processed with the resolution of ice chemistry samples (20 cm).

[10] Previous interpretations of the glaciochemistry data from the SDMA area, as available from shallow ice cores or snow pit samples [*Kreutz and Mayewski*, 1999], suggest that in addition to biogenic and continental dust components enhanced transport of marine air masses is responsible for the high concentration of sea-salt species (Na^+, Mg^{2+}, Cl^-). Earlier studies in Greenland and Antarctica set the methodological base for partitioning different sulfate source components from total sulfate measured in ice core samples [*Mayewski et al.*, 1986, 1990; *Legrand and Delmas*, 1987; *Legrand et al.*, 1988; *Wagenbach*, 1996; *Kreutz et al.*, 1999, 2000]. Several techniques exist to identify the portion of sulfate delivered from volcanic eruptions [*Zielinski et al.*, 1996b; *Cole-Dai et al.*, 1997; *Palmer et al.*, 2001]. To ensure comparability with the longest developed volcanochemistry record from the Northern Hemisphere (i.e., GISP2 ice core *Zielinski et al.*, 1994, 1996b, 1997b), we chose to apply the same methodology used to separate the volcanic component of the sulfate signal.

[11] Detection of volcanic events in ice cores is based on the observed sharp increase in sulfate concentration, often orders of magnitude above background level, following the volcanic eruption [*Zielinski*, 2000; *Mosley-Thompson et al.*, 2003]. This increase corresponds to observed trends in the stratosphere and troposphere measured by the COSPEC (correlation spectrometer) and the TOMS (total ozone mapping spectrometer] instruments [*Halmer et al.*, 2002]. Unfortunately, the magnitude of the sulfate spike in ice cores could be the same for a relatively small, local volcanic eruption in Antarctica or a large volcanic eruption that took place in lower latitudes. Spatial variability of the signal magnitude produced by the large 1815 eruption of Tambora is reported from several Antarctic ice cores [*Cole-Dai et al.*, 1997; *Dixon et al.*, 2004] and was attributed to "wind redistribution, changes in accumulation rates, and variations in the frequency and timing of snowfalls" [*Castellano et al.*, 2005]. In order to create a sulfate spike in the ice core glaciochemical record a large quantity of sulfate must be released during the volcanic eruption, transported to the deposition site, and preserved in the transformation from snow to ice. The signal could potentially be masked by sulfate contributed during permanent quiescent degassing from moderate and relatively constant global volcanic activity, biogenic, marine, and anthropogenic sources [*Halmer et al.*, 2002] and also by coarse sampling intervals [*Zielinski et al.*, 1996b]. In the SDMA area over the last several hundred years all sources of sulfate appear to be relatively stable with the exception of large explosive volcanic events [*Kreutz et al.*, 1999, 2000]. The long-term background fluctuations in the SDMA sulfate concentration are attributed to changes in atmospheric circulation systems over the Antarctic continent, sea-salt sulfate, and biogenic sulfate sources related to shoreline migration toward the ice core site [*Meyerson et al.*, 2006].

[12] We used two complimentary methods to separate sulfate signals associated with large eruptions. In the first method, we removed a portion of the sea-salt sulfate ($ssSO_4^{2-}$) from the total sulfate time series time series by using the procedure of *O'Brien et al.* [1995]. This technique uses all of the major ions found in the sea salt to calculate the most conservative (limiting) species. On the basis of the most conservative element the sulfate concentration is then calculated based on the known sea-salt ratio for major ions to SO_4^{2-} in seawater. Therefore this method allows calculation of the minimum possible sea-salt contribution and is probably more reliable for the estimation of minimum values compared for example to calculations that are solely based on the ratio of Na^+ to SO_4^{2-} [*Palmer et al.*, 2001]. Background levels of non-sea-salt sulfate ($nssSO_4^{2-}$) are estimated by adjusting the tension parameter of the robust spline fit curve [*Bloomfield and Steiger*, 1983] (Figure 3). With its low sensitivity to outliers, low-tension robust spline fit functions have been shown [*Meeker et al.*, 1995] to be a good tool for calculating the background levels of sulfate in the GISP2 ice core [*Mayewski et al.*, 1994; *Zielinski et al.*, 1994, 1995]. All positive signals with residuals from background levels exceeding threshold values of mean (μ) plus one standard deviation (1σ) (Figure 3) are used to select sulfate spikes caused by volcanic events (Figure 4 and Tables 1 and 2). In more conservative studies only a mean plus two standard deviations (2σ) of sulfate values in the time series were used to separate volcanic events [*Cole-Dai et al.*, 1997]. Volcanic signals were detected using an outlier signal selection algorithm [*Zielinski et al.*, 1994, 1995; *Cole-Dai et al.*, 1997] that is based on mean and standard deviation.

[13] The second method we use to develop the volcanic event time series is based on empirical orthogonal function (EOF) analyses [*Meeker et al.*, 1995, 1997]. The EOF analysis of glaciochemical time series allows the separation of time series of each measured ion into dimensionless orthogonal modes of variability [*Mayewski et al.*, 1994; *O'Brien et al.*, 1995; *Zielinski et al.*, 1997b] or empirical eigenvectors (Table 3). This technique is used to identify patterns of simultaneous variation and assumptions can be made that these subspaces correspond to different dynamic processes of the observed system [*von Storch and Zwiers*, 2001]. The interpretation of the association of the particular EOF (eigenvector) with a specific process contributing to processes captured in the SDMA ice core is based on

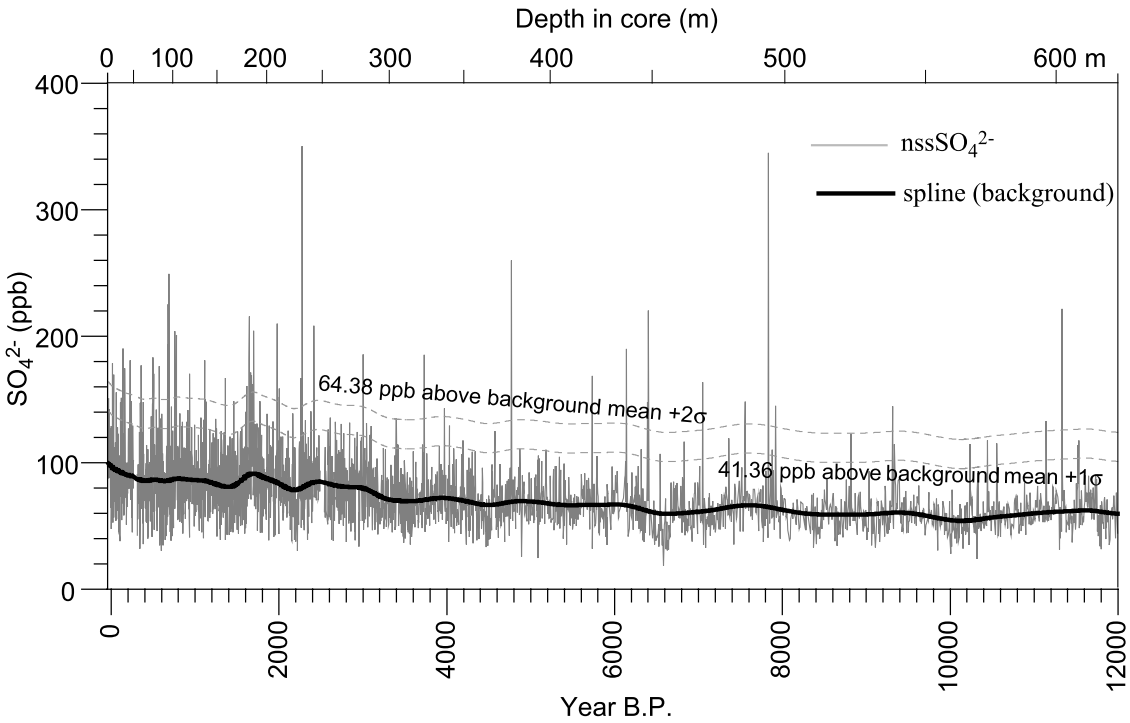

Figure 3. Concentration of non-sea-salt sulfate (nssSO_4^{2-}) for the last ~12 kyr in the SDMA ice core (0 year B.P. = 1950 C.E.). Low-tension robust spline fit curve corresponds to the background concentrations of nssSO_4^{2-} through this time period. Positive deviations from a background level exceeding mean of all positive residuals plus one standard deviation is interpreted as volcanic signals and summarized in Tables 1 and 2. Decrease in number of spikes with time, for the most part, is probably related to a decrease in sampling resolution in the deeper parts of the core.

investigation of correlations of ice chemistry species with air mass sources [*Mayewski et al.*, 1993; *Legrand and Mayewski*, 1997; *Kreutz et al.*, 1999, 2000; *Meyerson et al.*, 2006]. Earlier studies in the GISP2 ice core [*Zielinski et al.*, 1995, 1996b, 1997b] demonstrated that EOF analyses could successfully separate volcanically delivered sulfate aerosols from other sources of sulfate.

[14] Over the studied time interval raw SO_4^{2-} concentrations range from 39 to 390 μg/L with a mean around 96 μg/L. The mean Cl^- to mean Na^+ ratio for all samples is 1.87, which is very close to the sea-salt ratio of 1.86. The mean Na^+ value is 96.90 μg/L and mean SO_4^{2-} is 95.56 μg/L resulting in a Na^+: SO_4^{2-} ratio of 1.01 (sea-salt ratio is 3.99). It is intriguing that similar ratios are observed for mean atmospheric concentrations at Halley station Antarctica [*Rankin and Wolff*, 2003], which ultimately confirms that significant portions of marine aerosols are delivered to the SDMA location. Calculated non-sea-salt sulfate values (nssSO_4^{2-}) fluctuate from 19 μg/L to 351 μg/L (Figure 3). A robust spline curve with tension value 0.2 is used to estimate background levels of nssSO_4^{2-}. The mean of all positive residuals and one standard deviation equal 18.34 μg/L and 23.02 μg/L respectively. To develop our volcanochemistry record (Figure 4 and Tables 1 and 2) all signals exceeding 41.36 μg/L (mean of all positive residuals plus one standard deviation) are selected as volcanic (Figure 4). A number of these volcanic signals exceed 64.38 μg/L (mean of all positive residuals plus two standard deviations) (Figure 3 and Table 1). The largest sulfate spike signals (with residual 280 μg/L) occur 5881 B.C.E. Large residuals are also found during 325 B.C.E. (270 μg/L) and 1262 C.E. (163 μg/L).

[15] The EOF analyses of the SDMA time series of six major ions (Table 3) shows that 64% of the total variance for all ions is associated with EOF1. EOF1 explains 45% of total variance of SO_4^{2-}, 92% of Ca^{2+}, 87% of Mg^{2+}, 62% of Na^+, and is likely associated with sea salt. In EOF4 (6% of the total variance for the ion series) 25% of Na^+ is positively correlated with only 0.5% of the SO_4^{2-} signal. The likely explanation for this is that EOF4 sodium (and sulfate) is produced during the summer months. The observed chloride deficit can be contributed to the chloride depletion relative to sodium during the summer [see *Rankin and Wolff*, 2003] or postdepositional dechlorination observed in snow pits [*Rothlisberger et al.*, 2003]. EOF3 (10% of the total variance) reveals much (47%) of the volcanic portion of $SO4^{2-}$ with a small portion of the continental sulfate (positive correlation 0.19 with K^+). To exclude expected noise contributed by other sulfate sources (mainly biogenic emissions, quiescent volcanic degassing, and continental dust) only those sulfate spikes that exceed 36.33 μg/L (mean = 16.75, 1 standard deviation = 19.58) of all sulfate partitioned in EOF3 are selected as volcanic. The correlation coefficient of signals detected by robust spline and EOF methods is 0.9. Both robust spline and EOF methods detected 97 common signals. In addition, each statistical technique selected 27 separate events (Tables 1 and 2).

[16] We calculated volcanic sulfate depositional flux for each detected volcanic event by multiplying volcanic sulfate concentrations, length of ice sample, and ice density. We did

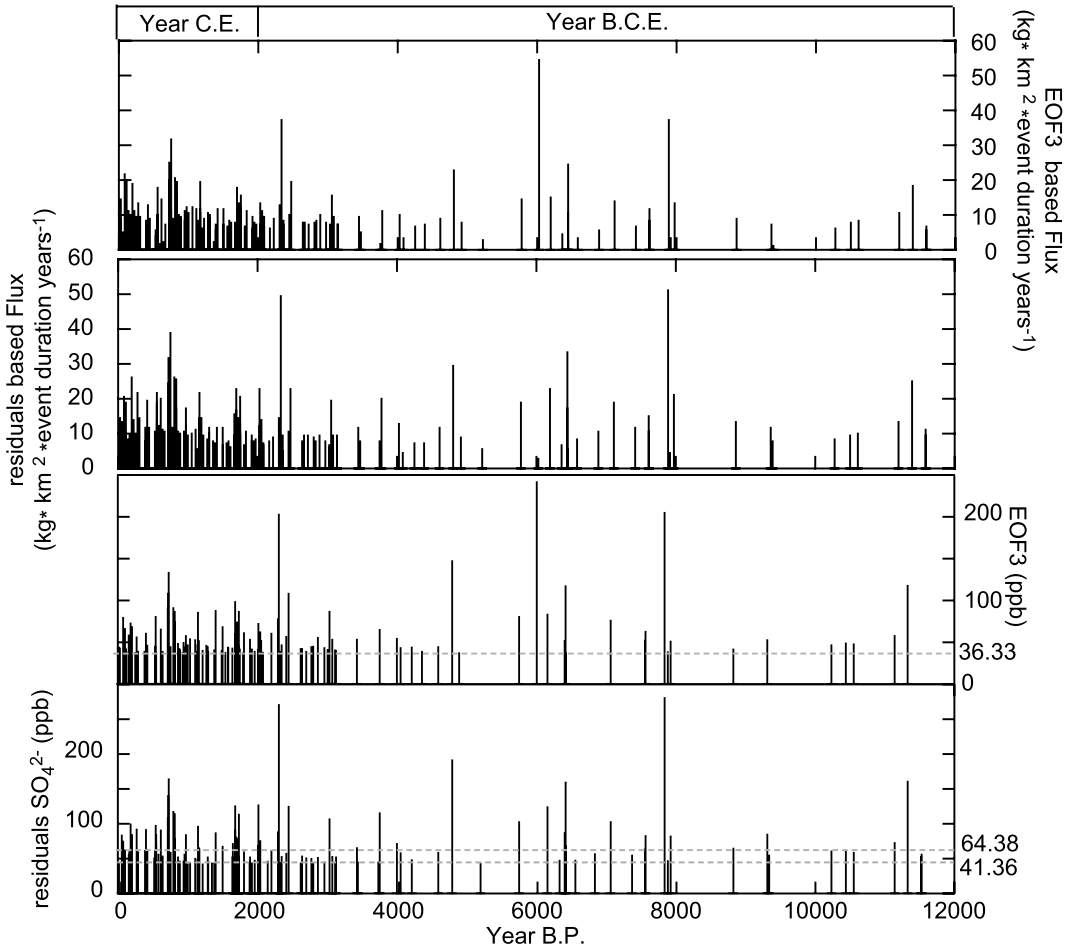

Figure 4. Comparison between volcanic SO_4^{2-} time series developed using EOF 3 and the low-tension robust spline technique (see text) for the last ~12 kyr. Please note that for flux-based signal calculation, magnitude deteriorates with depth compared to concentration values. The signal magnitude reduction is caused by coarser sampling resolution and potentially could influence threshold values used for selection of volcanic signals.

not account for annual layer thinning. The results are shown in Figure 4 and are also available as auxiliary material.[1] Several studies in Greenland [*Meeker et al.*, 1997] and Siple Dome [*Kreutz et al.*, 2000] demonstrated that in high-accumulation sites like GISP2 and SDMA there is no influence of snow accumulation rates measured in ice cores and snow pit or ice core ion concentrations. Nevertheless, the large uncertainty in calculating of sulfate depositional flux in coastal (high accumulation) areas could potentially propagate into calculations of the atmospheric loading from volcanic eruptions.

2.2. Tephra Fingerprinting

[17] As mentioned earlier, the timing of the sulfate signal and its magnitude helps in identifying the source of a volcanic eruption. Additional information on source can be obtained by means of ice core tephrochronology [*De Angelis et al.*, 1985; *Palais*, 1985; *Palais et al.*, 1989c, 1990, 1992; *Zielinski et al.*, 1995, 1997a, 1997b; *Zielinski and Germani*, 1998; *Zdanowicz et al.*, 1999; *Basile et al.*, 2001; *Dunbar et al.*, 2003]. To corroborate the validity of the volcanic time series derived from the ice chemistry record we analyze filtered particles from most of the samples adjacent to layers interpreted as volcanic using the electron microprobe. The morphology and composition of tephra particles found in the SDMA ice core allows geochemically "fingerprint" [*Dunbar et al.*, 2003] a source magmatic provenance or to identify specific volcanic eruption. Following the method of *Perkins et al.* [1995], a statistical distance function is used to assess the potential correlation of tephra particles with sources. This tephra correlation method involves calculation of the "Euclidean distance" function, (D, in standard deviation units) representing the degree of similarity between samples. Only samples with significant number of points (4–20 measurements) that represent similar population are used for correlation with sources.

[18] In order to select filters for the electron microprobe analysis we prepared optical slides for microscopy and scanned with an Olympus BX-40 optical microscope for the presence of tephra particles. An aliquot of the melted ice sample is centrifuged for 15 min, then 120 μL is withdrawn from the bottom and evaporated on a precleaned, preheated slide. Volcanic particles are separated from the remaining

[1] Auxiliary material is available at ftp://ftp.agu.org/apend/jd/2005jd006072.

Table 1. Volcanic Signals in the SDMA Ice Core Over the Last 2000 years and Possible Eruption Sources

Year C.E.(Duration, years)	Signal,[a] ppb	Volcanic Eruptions Possibly Associated With Detected Events[b]
1975 (2.8)	44 {43}	Fuego, Guatemala 1974 (VEI = 4)
1964 (1.9)	{42}	Agung, Indonesia 1963 (VEI = 5)
1936 (1.2)	**83**	Bristol Island, Antarctica 1936 (VEI = 2)[c]
1920 (3.1)	**74** {**79**}	Puyehue, Chile 1921 (VEI = 4)
1889 (2.2)	62 {**66**}	Lonquimay, Chile 1887–1889 (VEI = 3)
1887 (2.1)	{42}	Tarawera, New Zealand 1886 (VEI = 5)[d]
1883 (1.7)	{37}	Krakatau, Indonesia 1883 (VEI = 6)
1876 (3)	{41}	Cotopaxi, Ecuador 1877 (VEI = 4)[e]
1871 (2.6)	{38}	Deception Island, Antarctica 1871[c]
1839 (1.9)	55 {**58**}	Buckle Island, Antarctica 1839[c]
1831 (1.9)	59 {47}	Hodson, Antarctica 1831[c]
1809 (3.1)	**99** {**72**} A	Buckle Island, Pleiades, Antarctica[f]
1805 (3.0)	T	no match found
1804 (1.0)	A	Buckle Island, Antarctica[f]
1787 (3.2)	**84** {**68**}	no match found
1746 (2.6)	{37}	Cotopaxi, Ecuador 1744 (VEI = 4)
1724 (3.2)	**91** {56}	no match found
1707 (3.1)	59 {38}	Cerro Hudson, Chile, cal 2σ C.E. 1447(1732)1953[g]
1614 (1.9)	{39}	no match found
1601 (1.9)	61	Huaynaputina, Peru 1600 (VEI = 6)[h]
1592 (2.1)	**91** {**60**}	Raung, Java 1593 (VEI = 5)
1569 (2)	62 {46}	Billy Mitchell, Papua New Guinea, 2σ cal C.E. 1451(1539)1627 (VEI = 6)
1471 (1.9)	50	no match found
1462 (2.8)	47	El Misti, Peru 1438–1471(VEI = 3+)
1459 (1.8)	60 {45}	no match found
1450 (2.1)	**97** {**80**}	no match found
1448 (2.1)	55	Kuwae, Vanuatu, 145 ± 10 (VEI = 6)[i]
1445 (3.1)	**70** {37}	no match found
1443 (2.5)	**84**	no match found
1412 (2.1)	55	Pinatubo, 1450 ± 50 (VEI = 5)
1376 (2.6)	**90** {**65**}	no match found
1368 (2.5)	49	El Chichon, Mexico, 1σ cal C.E. 1320(1408)1433[j]
1346 (2.2)	53 {38}	Cerro Bravo, Columbia, 2σ cal C.E. 264(1305,1365,1386)1436
1278 (2.7)	**108** {**90**}	no match found
1271 (2.7)	**139** {**108**}	no match found
1262 (3)	**163** {**133**}	Mount Melbourne[k]
1259 (2.6)	45 {43}	Quilotoa, Ecuador 2σ cal C.E. 1160(1260)1360[e]
1234 (2)	58 {44}	Cotopaxi, Ecuador, 2σ cal C.E. 1024(1221)1376[e]
1193 (2.5)	**117** {**91**}	no match found
1186 (2.2)	43	El Chichon, Mexico, 1σ cal C.E. 1025(1220)1278[j]
1183 (2.5)	{37}	Cerro Bravo, Columbia, 2σ cal C.E. 996(1160)1279
1175 (2.7)	**78** {**74**}	no match found
1172 (2.9)	**114** {**86**}	no match found
1132 (2.7)	52 {48}	no match found
1111 (2.7)	{42}	no match found
1100 (2.7)	45 {40}	no match found
1061 (2.7)7	{37}	no match found
1052 (2.3)	45 {49}	no match found
1035 (2.5)	55 {43}	Cerro Hudson, Chile, cal 2σ C.E. 655(1004)1159[g]
1016 (2.4)	**84** {**57**}	no match found
991 (2.6)	41 {46}	no match found
958 (2.9)	44 {54}	no match found
879 (3.1)	50 {52}	Cotopaxi, Ecuador, soil below cal 2σ C.E. 665(885)1019[e]
857 (2.5)	{38}	Cerro Bravo, Columbia, 2σ cal C.E. 562(790,842,859)1160
847 (2.8)	48 {46}	no match found
837 (2.6)	**95** {**85**}	no match found
828 (2.8)	**64** {51}	no match found
820 (2.2)	63	no match found
773 (3)	42 {40}	El Chichon, Mexico, 1σ cal. C.E. 675(779,788)961[k]
723 (2.6)	{46}	no match found
702 (3)	51 {44}	no match found
695 (2.3)	44 {38}	no match found
640 (2.6)	43	Rabaul, Papua New Guinea, (VEI = 6), 2σ cal C.E. 427 (646) 804
607 (2.1)	{40}	El Chichon, Mexico, 1σ cal C.E. 441(553,600,614)662[j]
605 (1.9)	43	no match found
590 (1.8)	**86** {**87**}	no match found
497 (2.7)	{39}	El Chichon, Mexico, 1σ cal C.E. 256(385, 439, 459, 478, 510, 531)654[j]
488 (2.3)	**67** {**68**}	no match found
443 (2)	{37}	Ilopango, El Salvador 1σ cal C.E. 421(429)526[l]
409 (2.3)	{43}	Krakatau, Indonesia 416 C.E.
404 (2.2)	{43}	Cerro Hudson, Chile, 390 C.E.[m]
344 (2.1)	51 {43}	Melimoyu, Chile 350 ± 200 C.E.[n]
335 (3)	**71**	no match found

Table 1. (continued)

Year C.E.(Duration, years)	Signal,[a] ppb	Volcanic Eruptions Possibly Associated With Detected Events[b]
306 (2.8)	**90** {**60**}	no match found
304 (2.3)	**125** {**98**} A	Mount Melbourne
290 (2.2)	**80**	no match found
279 (2.3)	45 {41}	Cotopaxi, Ecuador, soil below, cal 2σ C.E. 4(245,310,315)537[e]
277 (2.1)	**78** {**74**}	no match found
275 (1.7)	54	no match found
267 (1.6)	61 {40}	no match found
265 (2.3)	**70** {**68**}	no match found
262 (2.6)	54 {47}	no match found
259 (2.7)	52 {44}	no match found
252 (2.6)	**113** {**86**}	no match found
239 (2.1)	{41}	El Chichon, Mexico, charcoal, 1σ cal C.E. 132(249)394[j]
190 (2)	{37}	Pico De Orizaba, Mexico, 2σ cal C.E. 67(131)243[o]
176 (2.2)	59 {**61**}	Taupo, New Zealand 180 C.E. (VEI = 6+)
94 (2.3)	43	Cotopaxi, Ecuador, soil below, 2σ cal B.C.E. 350(cal C.E.128)cal C.E.534[e]
91 (2.2)	51 {53}	no match found
67 (2.8)	43 {41}	no match found
21 (2)	47 {38}	Tacana, Mexico/Guatemala, 1σ cal B.C.E. 38 (cal C.E. 25–72)cal C.E. 216[p]

[a]Values larger than 1σ plus mean of all positive residuals (>41.36) in μg/L obtained by robust spline method are shown without brackets; values above 2σ plus mean of positive residuals (>64.38) are shown in bold. Curly braces are used to show values 1σ plus mean (>36.33) in μg/L of positive EOF3 values; Values above 2σ plus mean of positive EOF3 (>55.91) are shown in bold. See text for more information on methodology. T indicates when tephra was found, and A indicates that tephra is from Antarctic sources; see Table 4.

[b]Eruption information for this table is mainly based on the work by *Simkin and Siebert* [1994, 2002–2005] with some of the additional sources specifically shown. Calendar ages of the historical eruptions sometimes have degree of uncertainty indicated as a range of possible years. Accepted radiocarbon dates for the volcanic eruptions were recalibrated to conventional ages using Calib 4.3 calibration program intercepts method. All possible years are shown within 2σ intervals [*Stuiver et al.*, 1998]. The volcanic explosivity index (VEI) that was developed by *Newhall and Self* [1982] is shown if it was reported.

[c]*LeMasurier and Thomson* [1990].
[d]*Nairin* [1979].
[e]*Barberi et al.* [1995].
[f]*Dunbar et al.* [2003].
[g]*Naranjo and Stern* [1998].
[h]*Adams et al.* [2001]. See text for the discussion on how age of this event was estimated.
[i]*Monzier et al.* [1994].
[j]*Espíndola et al.* [2000].
[k]*Hawley et al.* [2003].
[l]*Dull et al.* [2001].
[m]*Haberle and Lumley* [1998].
[n]*Naranjo and Stern* [2004].
[o]*Hoskuldsson and Robin* [1993].
[p]*Macias et al.* [2000].

melted ice samples using 0.2 μm pore size Nuclepore (PC) polycarbonate membrane filters under a dust free laminar flow hood for a quantitative geochemical analysis using an electron microprobe. Tephra is transferred off the filter using a folded piece of double-stick tape and grains are finely polished until exposed on the mount for Cameca SX-100 electron microprobe analysis. Backscattered electron imagery (BSE) is used to select the best, microlite-free glass shards for quantitative analysis resulting in a small number of analyses for some samples. Major element composition is determined for up to 20 glass shards per sample (Table 4). Normalization to 100% weight analytical totals is used because the effort to use the largest possible beam size for each shard can result in a small overlap between the beam and epoxy surrounding the shard, resulting in a low analytical total. An accelerating voltage of 15 kV and a probe current of 10 nA are used with peak count times of 20 s for all elements with the exception of Na (40 s), F (100 s), Cl (40 s), and S (40 s). Background counts are obtained using one half the times used for peak counts. The largest possible electron beam size, that most closely matches to individual particle diameters, is used from preset beam sizes of 25, 20, 15, and 10 microns. Beam sizes smaller than 10 microns are avoided to minimize the volatilization of Na [*Nielsen and Sigurdsson*, 1981] which would result in low detection of Na but artificially elevated values for other elements [*Morgan and London*, 1996]. In limited cases, an elevated Cl content results from overlapping of the beam onto the epoxy. These anomalous Cl values are removed from the data set and Cl is not used in algorithms for "geochemical fingerprinting." However, for correlation purposes, we consider that a small number of good shard analyses is preferable to a larger number of points, some of which are suspect and decrease the precision of the data. Analytical precision, based on replicate analyses of certified reference material (NBS-610), is listed in Table 4. A number of standards, including feldspar, amphibole, and glass are run as unknowns in each analytical session to monitor calibration accuracy and interrun reproducibility.

[19] Overall, tephra-bearing horizons from SDMA contain small, angular shards. The number of shards per sample ranged widely, from many hundreds, to tens, to a single glass shard per sample. The largest shards averaged around 50 microns in diameter. The average shard size appears to be between 5 and 10 microns and overall the tephra is very well sorted, although no quantitative analysis of grain size was done. Some shards exhibit edges of bubbles and some contain microlites.

Table 2. Volcanic Signals in the SDMA Ice Core Over the 10,000 Years B.C.E. and Possible Eruption Sources

Period, years B.C.	List of Possible Volcanic Eruptions Indicated by Year[a]
0-2000	28[b] (2.8) **126** {**72**}, 34 (2.5) **68** {41}, 54 (2.8) **75** {**62**}, 71[c] (2.1) {51}, 92[d] (3) {37}, 161[e] (2.3) 46, 216 (1.5) 60 {**60**}, 309 (2.1) **87** {**77**}, 325 (2.4) **270** {**203**}, 339 (3.2) 44 {37}, 347 (2.5) {39}, 363[f] (2.5) 52 {46}, 431 (2.2) 57 {**56**}, 467 (3) **124** {**108**}, 636[g] (3.9) 43 {42}, 661 (3.2) 53 {42}, 722 (3.9) 50 {38}, 791[h] (2.9) 50 {44}, 821 (3) 42 {45}, 891 (3.5) 51 {55}, 980[i] (3) 44 {43}, 1025 (3.4) {40}, 1031 (2.7) {41}, 1054 (2.8) **106** {**86**}, 1094 (3) 52 {53}, 1133 (3.1) 44 {40}, 1147[j] (3.7) 52 {40}, 1334 (2.5) T, 1448 (4.3) **65** {53}, 1466[k] (2.8) 44, 1760 (3.6) 44, 1779 (3.6) **115** {**65**}, 1783[l] (4.3) A, 1805[m] (3.6) T, 1815 (2.9) T
2001–4000	2022[n] (3.8) **71** {54}, 2067[o] (3.0) A, 2080[p] (1.3) 58 {43}, 2242 (2.7) 48 {43}, 2387 (4.2) {38}, 2622[q] (4.4) 58 {44}, 2818 (2.8) **191** {**147**}, 2922 (3.4) {37}, 3230 (3.3) 42, 3782 (4.1) **102** {**80**}
4001–6000	4038 (6.5) {**241**}, 4190 (4.6) **124** {**83**}, 4368 (3.8) 47, 4443 (5.5) **86** {51}, 4454 (5.7) **159** {**117**}, 4456 (2.2) **67** {36}, 4594 (4.5) 47, 4877 (4.6) 56, 5100 (8.4) **102** {**76**}, 5412 (7.5) 54, 5601[r] (4.9) 63 {52}, 5607 (6) **82** {**62**}, 5881 (5) **280** {**205**}, 5928 (3.8) 46 {38}, 5970 (6.9) **81** {51}
6001–8000	6217[s] (14) A, 6231[t] (12) A, 6869[u] (7.3) 64 {41}, 7364 (4.6) **84** {52}, 7385[v] (4.8) 54, 7405[w] (6.1) T, 7756[x] (1.2) A, 7768[x] (15) A
8001–10,000	8283[y] (4.2) 60 {46}, 8495[z] (5.1) 62 {49}, 8606 (6.1) 58 {47}, 9193 (6.1) **72** {**57**}, 9216 (3.0)[aa] T, 9346[o] (3.7) A, 9382 (5.8) **160** {**117**}, 9574 (5.4) 52, 9584 (6) 56

[a]Calendar ages of the source eruptions sometimes have degree of uncertainty indicated as a range of possible years. Radiocarbon dates for the volcanic eruptions reported in the literature were recalibrated to conventional ages using Calib 4.2 calibration program intercepts method. All possible years are shown within 2σ intervals [*Stuiver et al.*, 1998].

[b]Each volcanic event is separated by a comma. The first number represents earliest year B.C.E. for the event in the ice core, the next number in parenthesis is a duration of the sampled interval, the next two numbers, if available, are the signal magnitude in ppb determined by robust spline and EOF (inside of the curly braces) methods, respectively. Values above 2σ plus mean for positive residuals and EOF3 time series are shown in bold. See text for more information on methodology.

[c]Cotopaxi, Ecuador, Layer 17, soil below 2σ cal B.C.E. 352(cal B.C.E. 46) cal C.E.126, *Barberi et al.* [1995].

[d]El Chichon, Mexico, Layer H, 2σ cal B.C.E. 191 (36, 5) cal C.E.112, *Espíndola et al.* [2000].

[e]Raoul Island, New Zealand, 2σ cal B.C.E. 393(199, 186, 184) cal C.E. 1 (VEI = 6), *Simkin and Siebert* [1994, 2002–2005].

[f]Atacazo, Ecuador, 2σ cal B.C.E. 764(403)212, *Simkin and Siebert* [1994, 2002–2005].

[g]El Chichon, Mexico, Layer I, 1σ cal B.C.E. 766(753, 699, 533)412, *Espíndola et al.* [2000].

[h]Cerro Hudson, Chile cal B.C.E. 810(790)770, *Haberle and Lumley* [1998].

[i]Sollipulli, Chile, cal B.C.E. 920 ± 90, *Gilbert et al.* [1996].

[j]El Chichon, Mexico, Layer J, 1σ cal B.C.E. 1415(1300, 1276, 1269)1124, *Espíndola et al.* [2000].

[k]Aguilera, Chile,< cal B.C.E. 1646 ± 230, *Kilian et al.* [2003].

[l]Mount Takahe, Antarctica.

[m]Mount Burney, Chile, cal B.C.E. 2304 ± 120, *Kilian et al.* [2003].

[n]Cerro Hudson, Chile (VEI = 6), cal B.C.E.1935[1890]1870, *Haberle and Lumley* [1998].

[o]The tephra is geochemically similar to BIt-302 tephra, Mount Berlin, Antarctica [*Wilch et al.*, 1999].

[p]El Chichon, Mexico, Layer K, 1σ cal B.C.E. 2171[2033]1932, *Espíndola et al.* [2000].

[q]Pico De Orizaba, Mexico, Avalos Layer, soil below cal 2σ B.C.E. 2902(2615, 2615, 2578)2210, *Dull et al.* [2001].

[r]Cerro Hudson, Chile, cal B.C.E. 5580, *Naranjo and Stern* [1998]; cal B.C.E. 5590, *Haberle and Lumley* [1998]; cal B.C.E. 5757 ± 185 − 5845 ± 131, *Kilian et al.* [2003].

[s]Mount Takahe, Antarctica.

[t]Mount Takahe, Antarctica (two 1–5 mm visible ash layers 21 cm apart).

[u]Mount Burney, Chile, tephra between two radiocarbon samples cal B.C.E. 7059 ± 17 and 7225 ± 111, *Kilian et al.* [2003].

[v]Mount Burney, Chile, tephra older cal B.C.E. 7225 ± 111, *Kilian et al.* [2003].

[w]South America?

[x]Mount Berlin, Antarctica.

[y]Yanteles, Cerro, cal B.C.E. 8350 ± 300, *Naranjo and Stern* [2004].

[z]Chaiten, Cerro, cal B.C.E. 8550 ± 200, *Naranjo and Stern* [2004].

[aa]Cerro Hudson, Chile, 1σ cal B.C.E. 10960[9110]9010, *Haberle and Lumley* [1998].

[20] Tephra compositions range from basanitic to trachytic to rhyolithic. Several samples exhibit a wide compositional range of as much as 10 wt % SiO_2. However, elements within these samples covary suggesting that the shards represent a coherent population (Table 4, SDMA-9008) that represents a distinct eruptive event rather than being a group of unrelated shards. In other cases individual shards, or several unrelated glass shards are observed in a sample (Table 4, SDMA-2433a and SDMA-2433b), so interpretation of the sources of these shards is less clear. These shards may represent large distant eruptions, small volume local events, or may simply be windblown material. The latter interpretation is suggested by the presence of a number of other particles including feldspar, quartz, mica, and clay minerals in these samples. Tephra is also found below 624 m in the SDMA ice core (A. Gow and D. Meese, personal communication, 2003) in addition to volcanic horizons detected by a borehole data logger method [*Bay et al.*, 2004].

2.3. Correlation of the Detected Volcanic Signals With Source Eruptions

[21] Despite the fact that the quantitative major element composition of tephra particles in Antarctic ice cores have been reported in a number of studies only a limited number of these reports have successfully identified the source of the volcanic eruptions with a confidence level compatible to traditional studies on terrestrial tephra layers. It is common for tephra samples from ice cores to have only a few glass shards with grain sizes in a range of several microns. This limits possible analytical methods for determination of major element composition because even the most advanced microprobe instruments produce measurements that are close to the instruments detection limits. Another aspect

Table 3. Joint Empirical Orthogonal Function Analysis

	Eigenvector Components				Percent Variance Explained				
Species	EOF1	EOF2	EOF3	EOF4	EOF1	EOF2	EOF3	EOF4	Sum
Ca^{2+}	0.96	−0.10	−0.18	−0.13	91.99	0.99	3.22	1.60	97.80
K^{+}	0.33	0.89	0.19	−0.23	11.15	79.94	3.48	5.38	99.95
Mg^{2+}	0.93	−0.17	−0.20	−0.09	87.26	2.89	3.85	0.88	94.87
Na^{+}	0.78	0.35	−0.12	0.50	61.51	12.43	1.44	24.57	99.94
Cl^{-}	0.95	−0.15	−0.08	−0.16	89.25	2.19	0.59	2.54	94.57
SO_4^{2-}	0.67	−0.27	0.69[b]	0.07	44.57	7.37	47.47	0.52	99.92
Total[a]					64.3	17.6	10.0	5.9	99.95

[a]Values are percent of total variance explained.
[b]Partitioned by EOF sulfate selected for the study.

of the problem is the sparse record of Antarctic volcanism which provides only a limited number of possible eruptions for correlation with known historical eruptions. Nevertheless, a unique overwhelmingly alkaline [*LeMasurier and Thomson*, 1990] composition of Antarctic tephra helps largely in identification of Antarctic volcanic provinces.

[22] Volcanic eruptions with volcanic explosivity index (VEI) [*Newhall and Self*, 1982] greater than four [*Halmer et al.*, 2002] from tropical and subtropical regions are considered as possible sources of the globally transported volcanic aerosols potentially detectable in the SDMA ice core. Although VEI does not necessarily relate to sulfur output of the resulting signal, eruptions that are big enough to warrant a VEI $\geq$ 4 are most likely to produce a signal detected in an ice core. The Smithsonian Institute reports [*Simkin and Siebert*, 2002–2005] that South America has 122 stratovolcanoes and matches Japan with the number of most documented volcanic eruptions with VEI $\geq$ 4. Unfortunately, the historical record starts only from the eruption of El Misti volcano sometime between 1438 and 1471 C.E. Without a doubt South America can be a major source for many sulfate signals in the SDMA ice core. In a search for possible source eruptions we also compared volcanic records developed from Greenland [*Zielinski et al.*, 1994, 1996b, 1997b; *Clausen et al.*, 1997; *Mosley-Thompson et al.*, 2003] and other Antarctic [*Langway et al.*, 1995; *Cole-Dai et al.*, 1997; *Palmer et al.*, 2001; *Basile et al.*, 2001; *Stenni et al.*, 2002; *Dunbar et al.*, 2003; *Castellano et al.*, 2004, 2005] ice cores as well as with a volcanic histories of south polar regions [*LeMasurier and Thomson*, 1990; *Smellie*, 1999].

[23] Because the dating error of sulfate signals in the SDMA ice core increases with age a confidence level for established correlations with source eruptions for each reported source eruptions is hard to estimate. It is certainly higher for signals linked to the possible source volcanic centers by tephra fingerprinting compared to eruption events correlated solely by sulfate signals found in the SDMA ice core.

3. Results

[24] A chronology of volcanism from the SDMA ice core for the last 12,000 years is combined from glaciochemical and tephra records (Tables 1, 2, and 4). Through our study we find that most tephra particles analyzed from the upper 600 m of the SDMA ice core are chemically consistent with a derivation from Antarctic volcanoes when compared with published source compositions [*Wilch et al.*, 1999; *Smellie*, 1999; *LeMasurier and Thomson*, 1990]. We were able to link SDMA tephra (Table 4) with sources from the Balenny Island, Pleiades, Mount Takahe (Figure 5a), and Mount Berlin volcanic centers (Figure 5b). In addition to Antarctic sources, several tephra layers in the SDMA ice core have compositions similar to South American volcanoes. Several sulfate signals in the SDMA ice core coincide with prehistoric eruptions of El Chichón, Mexico [*Espíndola et al.*, 2000]; Cerro Bravo, Columbia; Cotopaxi, Ecuador [*Simkin and Siebert*, 2002–2005]; and Cerro Hudson, Chile [*Naranjo and Stern*, 1998] volcanoes in addition to several global volcanic events from the low latitudes. Furthermore, only a few signals could be potentially linked with eruptions from New Zealand. We now discuss the most significant findings in the developed volcanological record for every 2 kyr interval chronologically over the last 12 kyr.

3.1. Time Interval 1–1975 C.E.

[25] Ninety-one events are detected in the SDMA ice core in this interval. From four tephra layers at 1809, 1805, 1804, and 304 C.E. (Tables 1 and 4), three layers are geochemically similar to volcanic rocks of Buckle Island and Mount Melbourne volcanic province, Antarctica. These 1809 C.E. and 304 C.E. Antarctic eruptions are also associated with large increases in sulfate levels in corresponding ice chemistry samples (Table 1). Finding tephra particles associated with recent Antarctic eruptions is not that surprising because sporadic evidence of Antarctic volcanism were observed during brief visits in earlier days of the Antarctic continent exploration [*LeMasurier and Thomson*, 1990]. Two basanitic tephra layers found at shallow depths of 33.61 and 34.60 m, in the SDMA ice core were already reported by *Dunbar et al.* [2003]. New refined ages of 1811 C.E. and 1804 C.E. respectively, for these tephra samples are based on the latest SDMA timescale [*Taylor et al.*, 2004]. The source volcanic centers for these tephra layers could be the Dry Valleys/Royal Society Range area where many basanitic vents are located. Alternatively, a sub-Antarctic volcanic area, such as Balleny Islands, that has produced basanitic material and has erupted recently [*Wright and Kyle*, 1990] could be provide potential tephra sources as well. Geochemically, no very satisfactory matches can be found for the mafic tephra found at 33.61, 34.45 and 34.6 meters in the SDMA ice core. The compositional match of the tephra with rock sampled at Balleny Islands is poor (D = 221 and 171), but analyses are of whole rock lava samples rather than the glassy component of pyroclastic material. Consequently, a good match would not necessarily be expected.

[26] We missed the Tambora event in the SDMA ice core due to heavily fractured ice but ITASE cores 01-5, 01-1, 00-4,

Table 4. Average Major Element Composition of Tephra From the SDMA Ice Core[a]

Sample	Depth	Age C.E.	N[b]	P_20_5	SiO_2	SO_2	TiO_2	Al_2O_3	MgO	CaO	MnO	FeO	Na_2O	K_2O	F	Cl
165	33.61	1811	4	0.63	44.33	0.11	3.92	15.15	5.83	12.83	0.22	11.8	3.51	1.37	0.17	0.12
SD[c]				0.04	0.48	0.02	0.17	0.26	0.45	0.31	0.02	0.53	0.38	0.11	0.29	0.05
166	33.75	1810	8	0.07	63.4	0.05	0.4	16.77	0.14	1.21	0.27	6.3	5.99	4.91	0.17	0.32
SD				0.02	0.51	0.02	0.08	0.27	0.04	0.05	0.03	0.55	1.25	0.64	0.11	0.1
171	34.45	1805	1	1.02	43.22	0.17	4.91	14.7	4.84	10.93	0.28	13.35	4.59	1.61	0.23	0.15
171	34.45	1805	1	0.67	46.01	0.09	3.47	16.07	5.55	11.38	0.21	11.54	3.49	1.4	0	0.12
171	34.45	1805	1	0.13	60.26	0.1	0.52	15.68	0.22	1.28	0.33	7.63	8.3	5.26	0	0.29
172	34.6	1804	9	0.78	42.74	0.13	4.64	14.81	6.02	11.7	0.2	13.13	4.03	1.57	0.16	0.08
SD				0.08	1.18	0.02	0.52	0.87	1.09	0.67	0.03	0.93	0.64	0.23	0.12	0.01
657c	182.76	304	1	0.78	54.38	0.18	2.08	14.78	2.4	6.2	0.25	11.95	3.71	2.94	0.36	-
657c	182.76	304	1	0.76	55.3	0.25	2.12	14.75	2.14	5.89	0.29	11.65	3.8	2.91	0.14	-
657c	182.76	304	1	0.69	55.95	0.17	1.97	15.96	1.67	5.06	0.17	10.76	5.15	2.29	0.16	-
657c	182.76	304	1	0.64	56.2	0.29	2.09	14.08	2.09	5.73	0.37	11.73	3.52	3.04	0.25	-
657c	182.76	304	1	0.49	59.9	0.11	1.36	15.82	1.44	4.09	0.21	8.53	4.16	3.55	0.35	-
657c	182.76	304	1	0.95	60.89	0.67	2.33	12.97	0.71	5.05	0.25	8.94	3.57	3.49	0.2	-
657c	182.76	304	1	0.33	63.14	0.3	0.9	15.38	0.59	3.28	0.26	7.97	3.85	3.72	0.28	-
657c	182.76	304	1	0.21	63.38	0.09	0.7	15.5	0.46	3.02	0.22	8.09	4.15	4.01	0.16	-
657c	182.76	304	1	0.06	68.06	0.28	0.28	14.72	0.02	2.72	0.04	4.38	4.11	5.22	0.13	-
2433a	298.528	−1334	2	0.12	63.85	0.1	0.43	19.8	4.4	2.35	0.01	5.37	0.4	2.96	0.2	-
SD				0.06	0.48	0.03	0.05	0.59	0.02	0.04	0.01	0.28	0.05	0.1	0.29	
2433b	298.528	−1334	8	0.06	77.1	0.04	0.08	12.46	0.26	0.65	0.05	1.23	2.05	5.91	0.09	-
SD				0.07	1.04	0.03	0.05	0.81	0.34	0.22	0.02	0.27	0.36	0.88	0.23	
2565	323.928	−1783	6	0.23	61.61	0.42	0.84	14.56	0.38	2.06	0.31	8.25	6.06	5.15	0.15	-
SD				0.13	0.67	0.21	0.05	0.31	0.05	0.35	0.06	0.27	0.26	0.14	0.09	
2571	325.12	−1805	1	0.13	67.88	0.59	0.65	14.46	1.54	3.7	0.16	5.34	4.55	1.01	0	-
2571	325.12	−1805	1	0.19	67.98	0.18	0.66	14.8	1.42	4.3	0.14	5.99	3.25	1.05	0.04	-
2571	325.12	−1805	1	0.21	68.18	0.15	0.67	14.85	1.39	4.15	0.2	5.44	3.6	1.12	0.04	-
2571	325.12	−1805	1	0.1	68.42	0.62	0.59	14.58	1.24	3.68	0.09	5.26	4.29	1.13	0	-
2571	325.12	−1805	1	0.14	68.84	0.42	0.41	14.27	1.02	3.21	0.16	5.18	3.87	1.18	1.3	-
2571	325.12	−1805	1	0.09	69.87	0.6	0.56	14.71	1.04	3.31	0.24	4.58	3.73	1.29	0	-
2571	325.12	−1805	1	0.08	71.16	0.17	0.46	16.02	0.76	3.01	0.18	5.17	1.3	1.68	0	-
2571	325.12	−1805	1	0.09	71.69	0.05	0.38	14.35	0.66	2.52	0.17	4.18	3.73	1.5	0.68	-
2571	325.12	−1805	1	0.09	72.35	1.48	0.32	13.4	0.4	2.44	0.17	3.58	3.53	1.38	0.86	-
2571	325.12	−1805	1	0.11	72.4	1.27	0.33	13.58	0.37	2.2	0.09	3.54	4.69	1.42	0	-
2571	325.12	−1805	1	0.24	72.6	1.44	0.24	13.89	0.41	2.54	0.19	3.45	3.81	1.19	0	-
2571	325.12	−1805	1	0.02	72.61	0.87	0.34	13.51	0.38	2.73	0.14	3.93	3.94	1.26	0.26	-
2571	325.12	−1805	1	0.03	73.3	0.02	0.39	14.27	0.42	2.5	0.19	3.74	3.79	1.36	0	-
2574	325.717	−1815	9	0.03	76.4	0.03	0.12	12.82	0.33	0.64	0.07	1.28	1.99	6.22	0.08	-
SD				0.03	1.1	0.01	0.05	0.55	0.24	0.29	0.04	0.24	0.46	0.93	0.1	
2648	340.129	−2067	12	1.87	45.79	0.3	3.69	14.79	5.14	8.94	0.25	13.7	4.27	1.13	0.14	-
SD				0.24	0.95	0.06	0.27	0.37	0.4	0.45	0.03	0.56	0.2	0.09	0.11	
9002c	503.584	−6217	15	0.18	61.55	0.14	0.87	14.86	0.41	1.8	0.33	8.63	6.07	4.99	0.17	-
std				0.04	0.51	0.02	0.07	0.21	0.04	0.12	0.03	0.41	0.6	0.15	0.08	
9006	503.874	−6231	16	0.17	60.93	0.14	0.89	14.76	0.38	1.77	0.34	8.93	6.5	4.99	0.19	-
SD				0.05	0.42	0.03	0.04	0.22	0.03	0.09	0.04	0.47	0.41	0.24	0.1	
9007	539.012	−7405	1	0.02	64.71	0.06	0.34	16.48	0.3	1.63	0.11	5.58	4.94	5.51	0.32	-
9007	539.012	−7405	1	0.07	65.13	0.03	0.33	16.69	0.14	1.63	0.17	5.4	5	5.13	0.28	-
9007	539.012	−7405	1	0.08	66.56	0.06	0.23	16.16	0.17	1.47	0.07	5.36	5.26	4.46	0.12	-
9007	539.012	−7405	1	0.03	72.45	0.03	0.15	13.51	0.05	0.51	0.14	3.49	4.94	4.02	0.66	-
9007	539.012	−7405	1	0	74.32	0.07	0.13	12.4	0.03	0.24	0.07	3.09	4.74	4.16	0.75	-
9007	539.012	−7405	1	0	73.98	0.09	0.11	12	0.25	0.31	0.11	3.56	4.56	4.26	0.76	-
9007	539.012	−7405	1	0.02	74.08	0.07	0.14	13.01	0	0.24	0.12	3.04	4.72	4.03	0.52	-
9007	539.012	−7405	1	0	74.66	0.07	0.14	12.3	0.01	0.2	0.1	2.98	4.73	4	0.82	-
9007	539.012	−7405	1	0.01	74.9	0.04	0.12	12.36	0.02	0.18	0.1	3.03	4.58	3.98	0.69	-
9007	539.012	−7405	1	0	75.55	0.01	0.16	12.35	0.02	0.22	0.05	3.18	3.81	4.15	0.49	-
9007	539.012	−7405	1	0.02	75.55	0.05	0.15	12.17	0	0.21	0.07	3	4.06	4.09	0.63	-
8004	550.02	−7756	20	0.1	62.56	0.12	0.48	14.27	0.04	1.54	0.34	9.1	6.4	4.84	0.16	-
SD				0.05	1.03	0.03	0.07	0.66	0.04	0.49	0.04	0.51	0.96	0.19	0.15	
4838	550.367	−7768	9	0.1	62.54	0.18	0.56	14.74	0.1	1.86	0.32	9.07	5.83	4.67	0.05	-
SD				0.05	1.29	0.06	0.13	0.55	0.05	0.18	0.04	0.98	1	0.38	0.06	
9008	596.952	−9216	1	0.23	55.31	0.02	1.15	12.99	3.18	7.37	0.29	14.06	4.65	0.65	0.1	-
9008	596.952	−9216	1	0.18	55.69	0	1.05	15.14	2.6	8.94	0.29	12.96	2.59	0.49	0.07	-
9008	596.952	−9216	1	0.07	56.29	0.04	0.84	13.32	6.16	7.33	0.31	13.07	2.23	0.34	0	-
9008	596.952	−9216	1	0.13	56.42	0.02	1.21	16.2	2.42	7.32	0.22	12.05	3.48	0.46	0.07	-
9008	596.952	−9216	1	0.15	56.48	0.07	1.02	15.95	2.46	8.53	0.27	11.1	3.09	0.55	0.33	-
9008	596.952	−9216	1	0.17	56.61	0.07	1.19	14.47	2.44	8.3	0.3	13.11	2.7	0.59	0.05	-
9008	596.952	−9216	1	0.2	57.5	0.04	1.21	13.18	2.87	6.92	0.27	13.12	3.9	0.58	0.2	-
9008	596.952	−9216	1	0.1	57.61	0.03	0.74	17.29	2.36	7.59	0.23	9.22	4.39	0.44	0	-
9008	596.952	−9216	1	0.15	57.81	0.07	1.03	15.6	2.64	7.42	0.25	10.81	3.6	0.54	0.08	-
9008	596.952	−9216	1	0.17	58.24	0.05	0.98	14.01	3.68	6.88	0.29	12.41	2.73	0.47	0.09	-
9008	596.952	−9216	1	0.21	58.49	0.04	1.16	14.91	2.2	7	0.31	11.92	3.16	0.6	0	-
9008	596.952	−9216	1	0.11	58.92	0.06	0.93	15.61	2.61	7.01	0.3	10.83	2.99	0.53	0.09	-
9008	596.952	−9216	1	0.09	64.18	0	0.62	14.08	2.23	5.74	0.24	8.65	3.49	0.68	0	-

Table 4. (continued)

Sample	Depth	Age C.E.	N[b]	P_2O_5	SiO_2	SO_2	TiO_2	Al_2O_3	MgO	CaO	MnO	FeO	Na_2O	K_2O	F	Cl
5086	601.235	−9346	6	0.07	63.42	0.19	0.46	14.28	0.02	1.35	0.32	9.06	5.9	4.79	0.13	-
SD				0.04	1.01	0.06	0.04	0.49	0.03	0.59	0.03	0.49	0.63	0.24	0.16	

[a]In cases when a mixed tephra population is found, all samples are given as opposed to the mean. Geochemical quantities are in weight percent. Analyses are normalized to 100 wt %. N equals number of analyses. Analytical precision, based on replicate analyses of standard reference materials of similar composition to the unknowns, are as follows (all in wt %): $SiO_2 \pm 0.47$, $TiO_2 \pm 0.03$, FeO ± 0.06, MnO ± 0.06, MgO ± 0.07, CaO ± 0.02, $Na_2O \pm 0.55$, $K_2O \pm 0.27$, $P_2O_5 \pm 0.02$, and Cl ± 0.07. SD indicates one standard deviation.
[b]Number of samples.

00-5, 99-1 collected from the region detected the sulfate signal from this eruption [*Dixon et al.*, 2004]. The sulfate spike at 1817 C.E., associated with the Tambora event, is present in the SDM94 ice core collected north of the SDMA ice core. Because SDM94 and SDMA ice cores have a similar sulfate glaciochemical record (K. J. Kreutz and P. A. Mayewski, unpublished data, 2005), and the cores are located only 2 km apart we are confident that the Tambora signal is present at the Siple Dome location despite the fact that it is not directly measured in SDMA glaciochemistry record.

[27] The compositionally different trachytic tephra analyzed in the SDMA ice core (sample SDMA-166 at 33.75 m depth with an age 1810 C.E.) appears to be geochemically similar to known eruption products from the Pleiades volcanic center but the Mount Melbourne volcanic center [*Kyle*, 1990; *Worner et al.*, 1989] is also potential candidate. Timing of this local, Antarctic eruption coincides with the

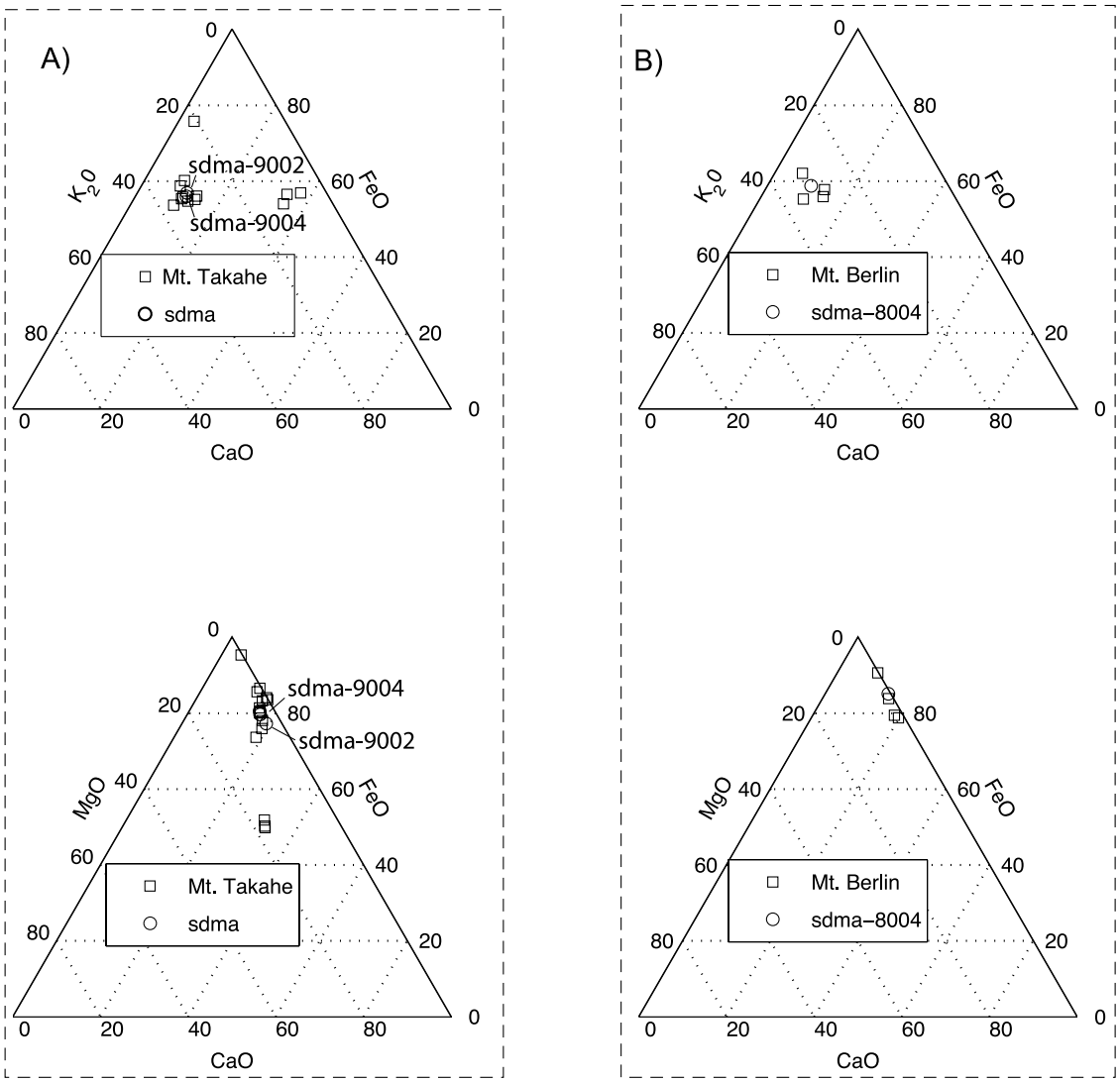

Figure 5. Ternary variation diagrams, which are useful for "fingerprinting" the glass shards found in the SDMA ice core with volcanic centers. Tephras from (a) Mount Takahe and (b) Mount Berlin are probably the best correlation examples in the SDMA record.

1809 C.E unknown eruption [*Mayewski et al.*, 1990; *Delmas et al.*, 1992; *Cole-Dai et al.*, 1997; *Palmer et al.*, 2001; *Mosley-Thompson et al.*, 2003] attributed previously by *Dai et al.* [1991] to a tropical region. Probably the idea of *Moore et al.* [1991] that two simultaneous eruptions in the Northern and Southern Hemisphere created the 1809 signal could be a better explanation of all existing data because the volcanic record developed from the Illimani ice core (Bolivia) does not show any signal 6 years before Tambora [*De Angelis et al.*, 2003]. If it was a large tropical event and if the Tambora signal is present, we should see the unknown 1809 signal as well.

[28] Increased volcanic activity around the 1600 C.E. Huaynaputina (Peru) eruption took place in 1600 C.E. [*de Silva and Zielinski*, 1998; *Adams et al.*, 2001] and is noted as a sulfate signal at 1601 C.E. The large Kuwae eruption of 1452 C.E. [*Monzier et al.*, 1994] which is among the largest volcanic eruptions recorded in many polar ice cores [*Mosley-Thompson and Thompson*, 1982; *Delmas et al.*, 1992] (see discussion by *Zielinski* [2000]) probably can be correlated with the 1448 or 1450 C.E. sulfate signals in the SDMA ice core. Our preference for the 1448 C.E. sulfate spike is based on several associations of large sulfate concentrations with tephra particles from the local eruption sources observed in SDMA. Until the age for the Kuwae eruption is better constrained both fall within the dating error. We did not find any tephra particles that would help us to link the sulfate signal with the eruption sources.

[29] The Siple Dome A and B ice cores offer new information that allows different interpretation for the nature of one of the largest sulfate spikes observed in Greenland, Antarctica, and the Canadian Arctic. The 1259 C.E. volcanic signal [*Hammer et al.*, 1980, 1984; *Langway et al.*, 1988, 1995; *Palais et al.*, 1992; *Zielinski et al.*, 1995; *Clausen et al.*, 1997; *Budner and Cole-Dai*, 2003] was previously attributed to the El Chichón eruption around 600 yr B.P. [*Tilling et al.*, 1984]. A revised stratigraphy of the El Chichón volcano [*Espíndola et al.*, 2000] rules out the El Chichón eruptions as a possible source for the 1259 signal. The Siple Dome B ice core (50 m from the SDMA borehole) has 1286 ± 35 years C.E. tephra that is compositionally similar to that of the Mount Melbourne volcano found at a similar depth (97.2 m) [*Dunbar et al.*, 2003] as a 1262 C.E. sulfate spike in the SDMA ice core. The same tephra layer is probably found at 1321 ± 25 C.E. and 1254 ± 2 C.E. respectively in Taylor [*Hawley et al.*, 2003] and Talos Domes [*Stenni et al.*, 2002], ice cores, Antarctica. The high-resolution record from the SDMA ice core shows two sulfate spikes at 1259 C.E. 1262 C.E. It may be possible that a combined signal from the 1259 C.E. (tropical) and 1262 C.E. (local) events was attributed originally to the sulfate spike around 1259 C.E. If we assume that the largest, 1262 C.E., sulfate signal is associated with the Mount Melbourne eruption and the 1259 C.E. signal to the Quilotoa eruption (VEI = 6), Ecuador [*Barberi et al.*, 1995] we can explain all of the latest data available. Comparison of available geochemical data from Quilotoa volcano [*Rosi et al.*, 2004] and glass shard samples from South Pole and GISP2 ice cores [*Palais et al.*, 1992] provide less conclusive correlations but they demonstrate that the El Chichón eruption is not correct source for this event. Because the age of Antarctic tephra is close to the 1259 spike we favor the idea of *Moore et al.* [1991] that a global increase in volcanic activity resulted in multiple moderate eruptions from globally distributed volcanoes and it created highly visible signals in ice cores from both hemispheres.

[30] The revised age for the Illopango eruption is close to the 443 C.E. sulfate signal [*Dull et al.*, 2001]. The sulfate signal at 409 C.E. is attributed to 416 C.E. eruption of the Krakatau volcano [*Simkin and Siebert*, 2002–2005]. A tephra layer at 182.76 m (304 C.E., sample SDMA-657) is chemically similar to the composition of trachytic lavas erupted from the summit of Mount Melbourne [*Worner et al.*, 1989]. The tephra composition suggests that it was derived from a zoned magma chamber (Table 4). Although no zoned eruptions are reported from Mount Melbourne the interpreted presence of a large, differentiating, shallow magma chamber at Mount Melbourne [*Worner et al.*, 1989] suggests that a zoned eruption is physically plausible. The range of compositions observed in sample SDMA-657 (Table 4) is coincident with the range of lava compositions observed at the summit of Mount Melbourne [*Worner et al.*, 1989]. The majority of moderate volcanic eruptions from New Zealand are not recorded in the SDMA ice core. Nevertheless one of the biggest caldera-forming eruptions (VEI = 6+) for the last 10 kyr is from Taupo volcanic center, New Zealand, around 180 C.E. [*Simkin and Siebert*, 2002–2005]. This is a potential candidate for the sulfate signal at 176 C.E.

3.2. Time Interval 0–2000 B.C.E.

[31] From the 35 volcanic events detected in the SDMA ice core in this interval, only four events contained tephra particles and these are found at 1334, 1783, 1805, and 1815 B.C.E. (Tables 2 and 4). One tephra layer is geochemically close to volcanic rocks of the Takahe volcano, Antarctica (Figure 5a) and another tephra is probably related to the largest eruption of Mount Burney, South America. Eight sulfate signals are probably associated with South and Central American volcanic eruptions and one or, possibly two, with activity of New Zealand volcanoes (Table 2). Sample SDMA-2433b (depth 298.53 m, age 1334 B.C.E.) is a normal calc-alkaline rhyolite. Its age is close to the large, rhyolitic, Waihimia eruption in New Zealand at 1350 B.C.E. [*Froggatt and Lowe*, 1990], but the composition of the Waihimia rhyolite is distinctly different than the layers in the SDMA ice core. The most dramatic difference is in the K_2O content, ~6 wt% K_2O in the ice core tephra and ~2.8 wt % in the Waihimia [*Dunbar*, 1988; *Blake et al.*, 1992]. It is unclear if tephra from New Zealand is present in this interval. At the 323.93 m depth in the core (SDMA-2565, 1783 B.C.E.), a tephra layer with a chemical composition similar to samples SDMA-9002c and SDMA-9006 (Table 4, D of 18 and 23, respectively) is observed. Although no eruptive event of this age has been recognized at this volcano we suggest that Mount Takahe may be the source of this tephra layer. The increased activity of the volcano may have produced an increase in sulfate at 1779 B.C.E. The chemical composition of SDMA 2571 (depth 325.12 m, age 1805 B.C.E.) sample has some similarity with tephra from Mount Burney (R. Kilian, personal communication, 2003), located in southern Chile. Glass from Mount Burney contains distinctly low K_2O [*Kilian et al.*, 2003]. The age estimate of the closest known eruption of Mount Burney is cal 2306?120 B.C.E.

based on peat growth rates and several radiocarbon dates [*Kilian et al.*, 2003]. This tephra is compositionally similar to the Mount Burney volcano but the large age difference between ages leaves linking this layer to the eruption of Mount Burney volcano problematic. Nevertheless, there is no known large eruption from Mount Burney volcano with similar ages so we suggest that further work must be conducted on correlation with Mount Burney eruptions.

3.3. Time Interval 2001–4000 B.C.E.

[32] Ten volcanic signals, including a single tephra horizon geochemically similar to the BIT-302 tephra layer [*Wilch et al.*, 1999] collected near Mount Berlin, Antarctica, were found in this interval.

3.4. Time Interval 4001–6000 B.C.E.

[33] Fifteen glaciochemical volcanic signals, but no tephra, were detected in this interval. The number of possible candidates from the record of global or South American eruptions that potentially can be linked with the SDMA sulfate record is quite limited from this time interval. The only possible identified source of volcanic sulfate at 5601 B.C.E. is one of the largest Holocene eruptions of Cerro Hudson volcano, Chile around 5590 B.C.E. [*Naranjo and Stern*, 1998; *Haberle and Lumley*, 1998; *Kilian et al.*, 2003]. Another potential candidate for this eruption is a sulfate signal at 5607 B.C.E.

3.5. Time Interval 6001–8000 B.C.E.

[34] Only eight volcanic events, five of which have visible tephra layers identified during the visual inspection of the SDMA ice core by A. Gow and D. Meese (unpublished data, 2003), were found from this interval. Four tephra layers are geochemically close to Mount Takahe and Mount Berlin volcanoes. One tephra layer and one sulfate signal probably came from South American volcanoes.

[35] Two visible tephra layers found at depths of 503.58 m (sample SDMA 9002c, Table 4) and 503.87 m (sample SDMA 9006, Table 4) with corresponding ages 6217 and 6231 B.C.E., respectively, correlate both chemically (Figure 5a) and chronologically with an episode of known volcanic activity of Mount Takahe volcano. The same tephra was probably detected in the Byrd core based on a reported ice flow modeled age of 7.5 kyr B.P. [*Palais et al.*, 1988] and $^{39}Ar/^{40}Ar$ age of 8.2?5.4 kyr B.P. [*Wilch et al.*, 1999]. Reanalyzed near-source pumice from this eruption compared with the tephra found in the SDMA ice core yields correlation D values between 11 and 14. Although these values are slightly outside the range that would ideally be considered to be robust correlations, the loss of Na during analysis of the very small particles found in the ice core may be responsible for the discrepancy.

[36] The 7756 B.C.E. tephra layer found at a depth of 550.02 meters (Sample SDMA 8004, Table 4) is chemically similar to tephra derived from Mount Berlin, West Antarctica. Although no exact chemical matches are found, the tephra layer shows a chemical affinity to a lava flow from the summit of Mount Berlin and to a set of tephra found at Mount Moulton (Figure 5b). The SDMA 9007 layer (depth 539.01 m, age 7405 B.C.E.) is chemically zoned, from calc-alkaline dacite to rhyolite, but is distinctly iron-rich and also chemically zoned, thus not compatible with derivation from a New Zealand eruption. This tephra may be the result of an unreported South American eruption.

3.6. Time Interval 8001–10,000 B.C.E.

[37] Nine volcanic events, including two visible tephra layers (A. Gow and D. Meese, personal communication, 2003) were found in this interval. One visible tephra layer geochemically close to Mount Berlin, Antarctica and another visible layer close to the tephra from Cerro Hudson volcano, Chile were found. The andesitic tephra layer at 9216 B.C.E., in terms of chemistry and chronology, may correlate with an eruption from Cerro Hudson, Chile [*Haberle and Lumley*, 1998; *Naranjo and Stern*, 1998]. The composition of the material from this Cerro Hudson eruption shows some chemical differences from this tephra, but it contains a distinctly high concentration of FeO, CaO, and low K_2O. The glass sampled in SDMA-9008 may be a slightly different phase of the eruption than those sampled by *Haberle and Lumley* [1998]. Tephra deposited from this eruption has only been recorded in the lake region to the west of the volcano suggesting an unusual transport pattern (C. Stern, personal communication, 2005). It is possible that a rather abnormal wind direction at the time of the eruption could account for the fast injection of the tephra cloud into the polar vortex around the Antarctic and rapid transport of the tephra particles to the SDMA ice core location. Another tephra layer with an age of 9346 B.C.E. is similar to the tephra composition at 7756 B.C.E. also derived from Mount Berlin, West Antarctica (Figure 5).

4. Frequency of Volcanic Eruptions in the Holocene

[38] The developed SDMA volcanic records provide estimates of volcanic activity over the studied interval. Observed fluctuations in the number of volcanic eruptions per century in the SDMA ice core compared with other volcanic records appear in Figure 6. Episodes of increased activity can be traced in several ice cores. The large increase in the number of volcanic events are recorded in the early part of the Holocene period in the GISP2 ice core as a result of deglaciation of the Northern Hemisphere [*Zielinski et al.*, 1996b] is not observed in the SDMA ice core. Nevertheless, we do see an increase in the number of visible tephra layers from Antarctic volcanoes around 7000 B.C. (Table 2). The link between volcanic activity and climate as a function of accumulated ice volume on the continents, lithosphere loading, and sea level change postulated by *Rampino et al.* [1979] has been corroborated by ice core records from Greenland [*Zielinski*, 2000]. As reported by *Castellano et al.* [2004, 2005] an increase in the number of volcanic eruptions for the last 2000 years is also observed in the SDMA ice core. We also observe gradual decrease in number of volcanic signals with depth. The detection of volcanic signals in the GISP2 ice core is different for high- and low-resolution time series [*Zielinski et al.*, 1996b].

5. Ramifications of the New SDMA-Derived Volcanic Record

[39] The detection of volcanic sulfate and tephra particles in the SDMA ice core provides a new 12,000 yr record of

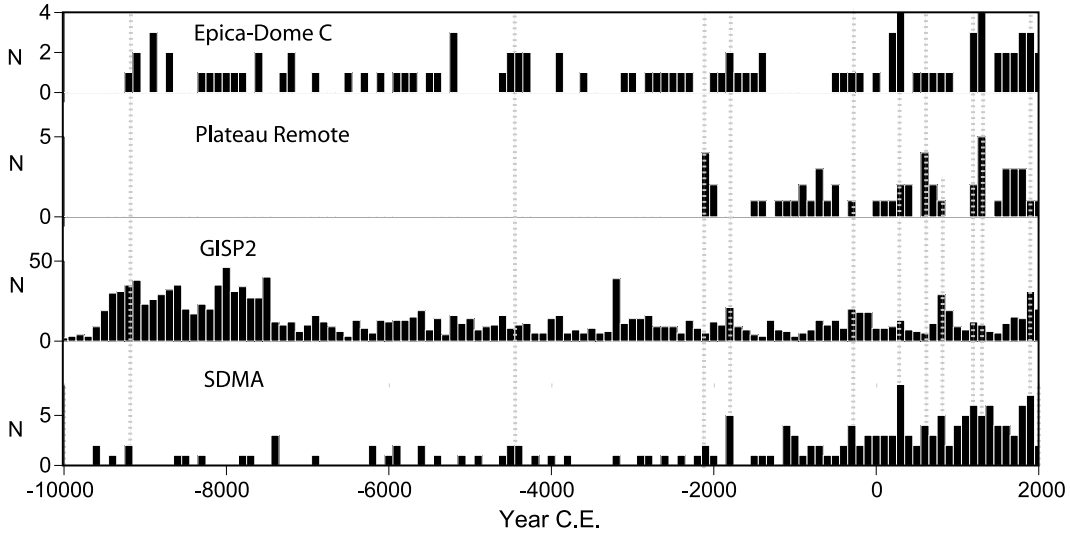

Figure 6. Comparison of the number of eruptions per century detected in the SDMA ice core with those found in the EPICA Dome C [*Castellano et al.*, 2004, 2005], Plateau Remote [*Cole-Dai et al.*, 2000] ice cores from Antarctica, and GISP2 ice core [*Zielinski et al.*, 1996b, 1997b] from Greenland. Please note the increase in the number of volcanic signals in the last 2000 years in all ice cores.

local, Antarctic, South American, New Zealand, and tropical eruptions. This volcanic record enhances the long-term history of Antarctic volcanism and highlights the importance of combining visual observations, simple optical microscopic examination of filtered samples, and ice chemistry measurements in the search for and interpretation of volcanic layers in ice cores.

[40] Tephra fingerprinting identified sources of tephra particles contributed by previously unknown Holocene eruptions of Mount Melbourne, The Pleiades, Balenny Island, Mount Berlin, Mount Melbourne and Mount Takahe volcanic centers (Antarctica), in addition to tephra layers possibly associated with Cerro Hudson and Mount Burney [Chile) volcanic eruptions. Detection of tephra layers from South American sources in the SDMA ice core provide new insights into the nature of atmospheric pathways from South America to Antarctica and the activity of the circumpolar vortex. Tephra fingerprinting also confirms historical observations that many Antarctic volcanoes are active and could be responsible for sulfate and tephra emissions on the continent. It certainly broadens recent assumptions [*Cosme et al.*, 2005] that the only presently active volcano in Antarctica responsible for sulfate pollution is Mount Erebus.

[41] Evaluation of sulfate spike signatures associated with the tephra in the SDMA volcanic record reveals specific patterns for Antarctic volcanic eruptions in the sulfate signal magnitude and the sulfate signal rate change. The ice chemistry samples adjacent to tephra layers from Mount Berlin, Mount Takahe, Mount Melbourne, Pleiades (East Antarctica), South Sandwich Islands, and Bransfield Strait volcanoes overall show associations with the large sulfate signals detected by both robust spline and EOF methods. In the SDMA ice core we observed a complex, nonlinear relationship between the magnitude of the eruption and the sulfate signal. Two sulfate signals at 1809 and 304 C.E. associated with tephra from Antarctic volcanoes show that local volcanic eruptions produce one of the largest sulfate spikes in the record, with residuals above 99 μg/L and EOF3 values above 73 μg/L. A close look at the results from the robust spline and EOF methods (Tables 1 and 2) reveals several differences in how both methods select volcanic signals. Not all volcanic spikes are always detected by both methods. We found that in the SDMA data set the robust spline technique is less sensitive to a smooth increase of sulfate concentrations over the several years usually observed during large tropical volcanic eruptions. It resulted in relatively moderate residual values for volcanic sulfate from tropical volcanic eruptions but these are also complicated by the abundance of biogenically produced sulfate related to the low elevation of the SDMA ice core site. In contrast, the EOF method takes into account changes in ice chemistry over the measured spectrum of all six ions over time (depth) in the ice core. An increase in sulfate species partitioned only in EOF3 is probably more likely associated with volcanically produced sulfate. It appears that future studies of the signatures of volcanic aerosols preserved ice cores should help to identify different modes of transport to the deposition area. Thus it should be possible to separate volcanic aerosols transported from Antarctic volcanic centers from volcanic products delivered via the stratosphere from tropical volcanoes based on glaciochemical signatures.

[42] We suggest that it is important to conduct tephra sampling in order to confirm volcanic events in sulfate based volcanic records, especially for ice core sites located close to the ocean with complex sulfate pathways and chemical cycles. Because the SDMA ice core is located close to the coast, we expect that the stratospheric component of the sulfate time series is mixed with a biogenic sulfate component transported by air masses from the sea [Meyerson et al., in press] and with volcanic aerosols associated with the same eruptions but transported via the troposphere. Our findings of a visible tephra layer from Mount Hudson volcano offer new light on possible tropospheric transport of volcanic products from the South American continent to the SDMA site in the past. Further

work is needed to understand this transport and possible separation of stratospheric and tropospheric sources in response to different climate forcing impacts.

[43] To implement a better algorithm for the separation of volcanic sulfate from other sources future fundamental work on sulfate sources and mechanisms of transport must be continued. Similar conclusions are drawn for future work on detection and analyses of the composition of the volcanic particles from low latitudes that are transported to the polar regions via the stratosphere. Better methods and analytical techniques for detection, sampling, and analyses have to be developed in order to provide robust tephra fingerprinting of these particles for reconstructing the source of volcanic eruptions. At this stage the SDMA volcanic record is a good example of the potential application of ice core based tephra fingerprinting because it helps to reconstruct the history of Antarctic volcanism. Once it is fully developed, we should be able to use it to separate sulfate spikes associated with local, Antarctic sources from signals that potentially can be linked with tropical and subtropical volcanic centers.

[44] **Acknowledgments.** This work was supported by grants OPP-9615167, OPP-0096305, and OPP-9526449 from the Office of Polar Programs, National Science Foundation. We thank many members of SDMA community for their valuable contributions to this manuscript and, particularly, R. Alley, D. Meese, and T. Gow for early access to core layer counting and dating data, G. W. Lamorey (Siple Dome Science Coordination Office; DRI), the 109th Air National Guard (Scotia, New York) for air transport and logistics, M. Wumkes (Glacier Data and Ice Core Drilling Services) and drillers from Polar Ice Coring Office, G. Hargreaves and J. Rhoades, M. S. Twickler (NICL), S. A. Story, D. Voisin (all UNH), and C. Corio (University of Maine) for freezer and ion chromatography laboratory assistance at University of Maine. Three anonymous reviewers made helpful suggestions on the manuscript.

References

Adams, N. K., S. L. de Silva, S. Self, G. Salas, S. Schubring, J. L. Permenter, and K. Arbesman (2001), The physical volcanology of the 1600 eruption of Huaynaputina, southern Peru, *Bull. Volcanol.*, *62*(8), 493–518, doi:10.1007/s004450000105.

Barberi, F., M. Coltelli, A. Frullani, M. Rosi, and E. Almeida (1995), Chronology and dispersal characteristics of recently (last 5000 years) erupted tephra of Cotopaxi (Ecuador): Implications for long-term eruptive forecasting, *J. Volcanol. Geotherm. Res.*, *69*, 217–239.

Basile, I., F. E. Grousset, M. Revel, J. R. Petit, P. E. Biscaye, and N. I. Barkov (1997), Patagonian origin of glacial dust deposited in East Antarctica (Vostok and Dome C) during glacial stages 2, 4 and 6, *Earth Planet. Sci. Lett.*, *146*(3), 573–590.

Basile, I., J. R. Petit, S. Touron, F. E. Grousset, and N. Barkov (2001), Volcanic layers in Antarctic (Vostok) ice cores: Source identification and atmospheric implications, *J. Geophys. Res.*, *106*, 31,915–31,931.

Bay, R. C., N. Bramall, and P. B. Price (2004), Bipolar correlation of volcanism with millenial climate change, *Proc. Natl. Acad. Sci. U. S. A.*, *101*(17), 6341–6345.

Blake, S., C. J. N. Wilson, I. E. M. Smith, and G. P. L. Walker (1992), Petrology and dynamics of the Waimihia mixed magma eruption, Taupo Volcano, New Zealand, *J. Geol. Soc. London*, *149*, 193–207.

Bloomfield, P., and W. L. Steiger (1983), Least absolute deviations: Theory, applications, and algorithms, *Prog. Probab. Stat.*, vol. 6, 349 pp., Springer, New York.

Brook, E. J., J. W. C. White, A. Schilla, M. L. Bender, J. Severinghaus, K. Taylor, R. Alley, and E. Steig (2005), Timing of millennial-scale climate change at Siple Dome, West Antarctica, during the last glacial period, *Quat. Sci. Rev.*, *24*, 1333–1343.

Budner, D. and J. Cole-Dai (2003), The number and magnitudes of large explosive volcanic eruptions between 904 and 1865 A.D.: Quanitative evidence from a new South Pole ice core, in *Volcanism and the Earth's Atmosphere*, *Geophys. Monogr. Ser.*, vol. 139, edited by A. Robock and C. Oppenheimer, pp. 165–176, AGU, Washington, D. C.

Castellano, E., S. Becagli, J. Jouzel, A. Migliori, M. Severi, J. P. Steffensen, R. Traversi, and R. Udisti (2004), Volcanic eruption frequency over the last 45 ky as recorded in Epica-Dome C ice core (East Antarctica) and its relationship with climatic changes, *Global Planet. Change*, *42*(1–4), 195–205.

Castellano, E., S. Becagli, M. Hansson, M. Hutterli, J. R. Petit, M. R. Rampino, M. Severi, J. P. Steffensen, R. Traversi, and R. Udisti (2005), Holocene volcanic history as recorded in the sulfate stratigraphy of the European Project for Ice Coring in Antarctica Dome C (EDC96) ice core, *J. Geophys. Res.*, *110*, D06114, doi:10.1029/2004JD005259.

Ciais, P., J. Jouzel, J. R. Petit, V. Lipenkov, and J. W. C. White (1994), Holocene temperatute variations inferred from six Antarctic ice cores, *Ann. Glaciol.*, *20*, 427–436.

Clausen, H. B., C. U. Hammer, C. S. Hvidberg, D. Dahl-Jensen, J. P. Steffensen, J. Kipfstuhl, and M. Legrand (1997), A comparison of the volcanic records over the past 4000 years from the Greenland Ice Core Project and Dye 3 Greenland Ice Cores, *J. Geophys. Res.*, *102*, 26,707–26,723.

Cole-Dai, J., E. Mosley-Thompson, and L. G. Thompson (1997), Annually resolved Southern Hemisphere volcanic history from two Antarctic ice cores, *J. Geophys. Res.*, *102*, 16,761–16,771.

Cole-Dai, J., E. Mosley-Thompson, S. P. Wight, and L. G. Thompson (2000), A 4100-year record of explosive volcanism from an East Antarctica ice core, *J. Geophys. Res.*, *105*, 24,431–24,441.

Cosme, E., F. Hourdin, C. Genthon, and P. Martinerie (2005), Origin of dimethylsulfide, non-sea-salt sulfate, and methanesulfonic acid in eastern Antarctica, *J. Geophys. Res.*, *110*, D03302, doi:10.1029/2004JD004881.

Dai, J., E. Mosley-Thompson, and L. G. Thompson (1991), Ice core evidence for an explosive tropical volcanic eruption 6 years preceding Tambora, *J. Geophys. Res.*, *96*, 17,361–17,366.

De Angelis, M., L. Fehrenbach, C. Jehanno, and M. Maurette (1985), Micrometre-sized volcanic glasses in polar ices and snows, *Nature*, *317*, 52–54.

De Angelis, M., J. Simões, H. Bonnaveira, J.-D. Taupin, and R. J. Delmas (2003), Volcanic eruptions recorded in the Illimani ice core (Bolivia): 1918–1998 and Tambora periods, *Atmos. Chem. Phys. Discuss.*, *3*, 2427–2463.

Delmas, R. J., S. Kirchner, J. M. Palais, and J.-R. Petit (1992), 1000 years of explosive volcanism recorded at the South Pole, *Tellus, Ser. B*, *44*, 335–350.

de Silva, S. L., and G. A. Zielinski (1998), Global Influence of the AD 1600 eruption of Huaynaputina, Peru, *Nature*, *393*, 455–458.

Dixon, D., P. A. Mayewski, S. Kaspari, K. Kreutz, G. Hamilton, K. Maasch, S. Sneed, and M. Handley (2004), A 200-year sulfate record from 16 Antarctic ice cores and associations with Southern Ocean sea ice extent, *Ann. Glaciol.*, *39*, 545–556.

Dull, R. A., J. R. Southon, and P. Sheets (2001), Volcanism, ecology, and culture: A reassessment of the Volcán Ilopango TBJ eruption in the Southern Maya Realm, *Lat. Am. Antiquity*, *12*(1), 25–44.

Dunbar, N. W. (1988), Pre-eruptive volatile contents and degassing systematics of rhyolitic magmas from the Taupo Volcanic Zone, New Zealand, Ph.D. thesis, N.M. Inst. of Min. and Technol., Socorro.

Dunbar, N. W., G. A. Zielinski, and D. T. Voisin (2003), Tephra layers in the Siple Dome and Taylor Dome Ice Cores, Antarctica: Sources and correlations, *J. Geophys. Res.*, *108*(B8), 2374, doi:10.1029/2002JB002056.

EPICA Community Members (2004), Eight glacial cycles from an Antarctic ice core, *Nature*, *429*, 623–628, doi:10.1038/nature02599.

Espíndola, J. M., J. L. Mac'as, R. I. Tilling, and M. F. Sheridan (2000), Volcanic history of El Chichón Volcano (Chiapas, Mexico) during the Holocene, and its impact on human activity, *Bull. Volcanol.*, *62*(2), 90–104.

Froggatt, P. C., and D. J. Lowe (1990), A review of late Quaternary silicic and some other tephra formations from New Zealand: Their stratigraphy, nomenclature, distribution, volume and age, *N.Z.J. Geol. Geophys.*, *33*, 89–109.

Gilbert, J. S., M. V. Stasiuk, S. J. Lane, C. R. Adam, M. D. Murphy, R. S. J. Sparks, and J. A. Naranjo (1996), Non-explosive, constructional evolution of the ice-filled caldera at Volcán Sollipulli, Chile, *Bull. Volcanol.*, *58*(1), 67–83.

Haberle, S. G., and S. H. Lumley (1998), Age and origin of tephras recorded in postglacial lake sediments to the west of the southern Andes, 44 degrees S to 47 degrees S, *J. Volcanol. Geotherm. Res.*, *84*(3–4), 239–256.

Halmer, M. M., H. U. Schmincke, and H. F. Graf (2002), The annual volcanic gas input into the atmosphere, in particular into the stratosphere: A global data set for the past 100 years, *J. Volcanol. Geotherm. Res.*, *115*, 511–528, doi:10.1016/S0377-0273(01)00318-3.

Hamilton, G. S. (2002), Mass balance and accumulation rate across Siple Dome, West Antarctica, *Ann. Glaciol.*, *35*, 102–106.

Hammer, C. U. (1983), Initial direct current in the build up of space charges and the acidity of ice cores, *J. Phys. Chem.*, *87*(21), 4099–4103.

Hammer, C. U. (1984), Traces of Icelandic eruptions in the Greenland ice sheet, *Joekull*, *34*, 51–65.
Hammer, C. U., H. B. Clausen, and W. Dansgaard (1980), Greenland ice sheet evidence of post-glacial volcanism and its climatic impact, *Nature*, *288*, 230–235.
Han, J., Z. Xie, F. Dai, and W. Zhang (1999), Volcanic eruptions recorded in an ice core from Collins Cap, King George Island, Antarctica, *Ann. Glaciol.*, *29*, 121–125.
Hawley, R. L., E. D. Waddington, D. L. Morse, N. W. Dunbar, and G. A. Zielinski (2003), Dating firn cores by vertical strain measurements, *J. Glaciol.*, *48*(162), 401–406.
Hoskuldsson, A., and C. Robin (1993), Late Pleistocene to Holocene eruptive activity of Pico de Orizaba, eastern Mexico, *Bull. Volcanol.*, *55*, 571–587.
Jouzel, J., et al. (2001), A new 27 ky high resolution East Antarctic climate record, *Geophys. Res. Lett.*, *28*(16), 3199–3202.
Karlöf, L., et al. (2000), A 1500 year record of accumulation at Amundsenisen western Dronning Maud Land, Antarctica, derived from electrical and radioactive measurements on a 120 m ice core, *J. Geophys. Res.*, *105*, 12,471–12,483.
Kilian, R., M. Hohner, H. Biester, H. J. Wallrabe-Adams, and C. Stern (2003), Holocene peat and lake sediment tephra record from the southernmost Chilean Andes (53–55°S), *Rev. Geol. Chile*, *30*(1), 23–37.
Kreutz, K. J., and P. A. Mayewski (1999), Spatial variability of Antarctic surface snow glaciochemistry: Implications for paleoatmospheric circulation reconstructions, *Antarct. Sci.*, *11*(1), 105–118.
Kreutz, K. J., P. A. Mayewski, M. S. Twickler, S. I. Whitlow, J. W. C. White, C. A. Shuman, C. R. Raymond, H. Conway, and J. R. McConnell (1999), Seasonal variations of glaciochemical, isotopic, and stratigraphic properties in Siple Dome, Antarctica surface snow, *Ann. Glaciol.*, *29*, 1–7.
Kreutz, K. J., P. A. Mayewski, L. D. Meeker, M. S. Twickler, and S. I. Whitlow (2000), The effect of spatial and temporal accumulation rate variability in West Antarctica on soluble ion deposition, *Geophys. Res. Lett.*, *27*(16), 2517–2520.
Kyle, P. R. (1990), Melbourne volcanic province, in *Volcanoes of the Antarctic Plate and Southern Oceans*, *Antarct. Res. Ser.*, vol. 48, edited by W. E. LeMasurier and J. W. Thompson, pp. 48–80, AGU, Washington, D. C.
Kyle, P. R., P. A. Jezek, E. Mosley-Thompson, and L. G. Thompson (1981), Tephra layers in the Bird station ice core and the Dome C ice core, Antarctica and their climatic importance, *J. Volcanol. Geotherm. Res.*, *11*, 29–39.
Langway, C. C., Jr., H. B. Clausen, and C. U. Hammer (1988), An interhemispehiric time-marker in ice cores from Greenland and Antarctica, *Ann. Glaciol.*, *10*, 102–108.
Langway, C. C., Jr., K. Osada, H. B. Clausen, C. U. Hammer, and H. Shoji (1995), A 10-century comparison of prominent bipolar volcanic events in ice cores, *J. Geophys. Res.*, *100*, 16,241–16,248.
Legrand, M., and R. J. Delmas (1987), A 220-year comntinuous record of volcanic H_2SO_4 in the Antarctic ice sheet, *Nature*, *327*, 671–676.
Legrand, M., and P. A. Mayewski (1997), Glaciochemistry of polar ice cores: A review, *Rev. Geophys.*, *35*, 219–243.
Legrand, M. R., R. J. Delmas, and R. J. Charlson (1988), Climate forcing implications from Vostok ice-core sulfate data, *Nature*, *334*, 418–420.
LeMasurier, W. E., and J. W. Thomson (Eds.) (1990), *Volcanoes of the Antarctic Plate and Southern Oceans*, *Antarct. Res. Ser.*, vol. 48, 487 pp., AGU, Washington, D. C.
Macias, J. L., J. M. Espindola, A. Garcia-Palomo, K. M. Scott, S. Hughes, and J. C. Mora (2000), Late Holocene Peléan-style eruption at Tacaná volcano, Mexico and Guatemala: Past, present, and future hazards, *Geol. Soc. Am. Bull.*, *112*(8), 1234–1249.
Mayewski, P. A., W. B. Lyons, M. J. Spencer, M. Twickler, W. Dansgaard, B. Koci, C. I. Davidson, and R. E. Honrath (1986), Sulfate and nitrate concentrations from a South Greenland ice core, *Science*, *232*, 975–977.
Mayewski, P. A., M. J. Spencer, W. B. Lyons, and M. S. Twickler (1987), Seasonal and spatial trends in south Greenland snow chemistry, *Atmos. Environ.*, *21*(4), 863–869.
Mayewski, P. A., W. B. Lyons, M. J. Spencer, M. Twickler, C. F. Buck, and S. Whitlow (1990), An ice-core record of atmospheric response to anthropogenic sulphate and nitrate, *Nature*, *346*, 554–556.
Mayewski, P. A., L. D. Meeker, S. Whitlow, M. S. Twickler, M. C. Morrison, R. B. Alley, P. Bloomfield, and K. Taylor (1993), The atmosphere during the Younger Dryas, *Science*, *261*, 195–197.
Mayewski, P. A., et al. (1994), Changes in atmospheric circulation and ocean ice cover over the North Atlantic region during the last 41,000 years, *Science*, *263*, 1747–1751.
Mayewski, P. A., L. D. Meeker, M. S. Twickler, S. I. Whitlow, Q. Yang, and M. Prentice (1997), Major features and forcing of high-latitude Northern Hemisphere atmospheric circulation using a 11,0000-year-long glaciochemical series, *J. Geophys. Res.*, *102*, 26,345–26,366.
Meeker, L. D., P. A. Mayewski, and P. Bloomfield (1995), A new approach to glaciochemical time series analyses, in *Ice Core Studies of Global Biogeochemical Cycles: Proceedings of the NATO Advanced Research Workshop on Biogeochemical Cycling*, *NATO ASI Ser., Ser. I*, vol. 30, edited by R. Delmas, pp. 383–400, Springer, New York.
Meeker, L. D., P. A. Mayewski, M. S. Twickler, and S. I. Whitlow (1997), A 11,0000-year-old history of change in continental biogenic emissions and related atmospheric circulation inferred from the Greenland Ice Sheet Project Ice Core, *J. Geophys. Res.*, *102*, 26,489–26,504.
Meyerson, E. A., et al. (2006), Examination of major Holocene climate change events in ice cores from West Antarctica (Siple Dome), East Antarctica (Taylor Dome), and Greenland (GISP2), *Holocene*, in press.
Monzier, M., C. Robin, and J. P. Eissen (1994), Kuwae (1425): The forgotten caldera, *J. Volcanol. Geotherm. Res.*, *59*, 207–218.
Moore, J. C., R. Mulvaney, and J. G. Paren (1989), Dielectric stratigraphy of ice: A new technique for determining total ionic concentrations in polar ice cores, *Geophys. Res. Lett.*, *16*, 1177–1180.
Moore, J. C., H. Narita, and N. Maeno (1991), A continuous 770-year record of volcanic activity from East Antarctica, *J. Geophys. Res.*, *96*, 17,353–17,359.
Morgan, G. B., and D. London (1996), Optimizing the electron microprobe analysis of hydrous alkali aluminosilicate glasses, *Am. Mineral.*, *81*, 1176–1185.
Mosley-Thompson, E., and L. G. Thompson (1982), Nine centuries of microparticle deposition at the South Pole, *Quat. Res.*, *17*(1), 1–13.
Mosley-Thompson, E., J. Dai, L. G. Thompson, P. M. Grootes, J. K. Arbogast, and J. F. Paskievitch (1991), Glaciological studies at Siple Station (Antarctica): Potential ice core paleoclimatic record, *J. Glaciol.*, *37*, 11–22.
Mosley-Thompson, E., T. A. Mashiotta, and L. G. Thompson (2003), High resolution ice core records of late Holocene volcanism: Current and future contributions from the Greenland PARCA cores, in *Volcanism and the Earth's Atmosphere*, *Geophys. Monogr. Ser.*, vol. 139, edited by A. Robock and C. Oppenheimer, pp. 153–164, AGU, Washington, D. C.
Nairin, I. A. (1979), Rotomahana-Waimangu eruption 1886: Base surge and basalt magma, *N. Z. J. Geol. Geophys.*, *22*, 363–378.
Naranjo, J. A., and C. R. Stern (1998), Holocene explosive activity of Hudson Volcano, southern Andes, *Bull. Volcanol.*, *59*, 291–306.
Naranjo, J. A., and C. R. Stern (2004), Holocene tephrochronology of the southernmost part (42°30′–45°S) of the Andean southern volcanic zone, *Rev. Geol. Chile*, *31*(2), 225–240.
Newhall, C., and S. Self (1982), The volcanic explosivity index (VEI): An estimate of explosive magnitude for historical volcanism, *J. Geophys. Res.*, *87*, 1231–1238.
Nielsen, C. H., and H. Sigurdsson (1981), Qualitative methods for electron microprobe analysis of sodium in natural and synthetic glasses, *Am. Mineral.*, *66*, 547–552.
Ninkovich, D., R. S. J. Sparks, and M. J. Ledbetter (1978), The exceptional magnitude and intensity of the Toba eruption, Sumatra: An example of the use of deep-sea tephra layers as a geological tool, *Bull. Volcanol.*, *41*, 286–298.
O'Brien, S. R., P. A. Mayewski, L. D. Meeker, D. A. Meese, M. S. Twickler, and S. I. Whitlow (1995), Complexity of Holocene climate as reconstructed from the Greenland ice core, *Science*, *270*, 1962–1964.
Oppenheimer, C. (2002), Limited global change due to the largest known Quaternary eruption, Toba 74 kyr BP?, *Quat. Sci. Rev.*, *21*, 1593–1609.
Palais, J. M. (1985), Particle morphology, composition and associated ice chemistry of tephra layers in the Byrd ice core: Evidence for hydrovolcanic eruptions, *Ann. Glaciol.*, *7*, 42–48.
Palais, J. M., P. R. Kyle, E. Mosley-Thompson, and E. Thomas (1987), Correlation of 3200 year old tephra in ice cores from Vostok and South pole stations, Antarctica, *Geophys. Res. Lett.*, *14*, 804–807.
Palais, J. M., P. R. Kyle, W. C. McIntosh, and D. Seward (1988), Magmatic and phreatomagmatic volcanic activity at Mount Takahe, West Antarctica based on tephra layers in the Byrd ice core and field observations at Mt. Takahe, *J. Volcanol. Geotherm. Res.*, *35*, 295–317.
Palais, J. M., R. Chuan, and M. Spencer (1989a), Soluble and insoluble impurities in snow samples from Ross Island, Antarctica, *Antarct. J. U. S.*, *24*(5), 89–91.
Palais, J. M., J.-R. Petit, C. Lorius, and Y. S. Korotkevich (1989b), Tephra layers in the Vostok ice core: 16,0000 years of Southern Hemisphere volcanism, *Antarct. J. U. S.*, *24*(5), 98–99.
Palais, J. M., S. Kirchner, and R. Delmas (1989c), Identification and correlation of volcanic eruption horizons in a 1,000-year ice-core record from the South Pole, *Antarct. J. U. S.*, *24*(5), 101–104.
Palais, J. M., S. Kirchner, and R. Delmas (1990), Identification of some global volcanic horizons by major element analysis of fine ash in Antarctic ice, *Ann. Glaciol.*, *14*, 216–220.

Palais, J. M., M. S. Germani, and G. A. Zielinski (1992), Inter-hemispheric transport of volcanic ash from a 1259 A.D. volcanic eruption to the Greenland and Antarctic ice sheets, *Geophys. Res. Lett.*, *19*(8), 801–804.

Palmer, A. S., T. D. van Ommen, M. A. J. Curran, V. Morgan, J. M. Souney, and P. A. Mayewski (2001), High-precision dating of volcanic events (A.D. 1301–1995) using ice cores from Law Dome, Antarctica, *J. Geophys. Res.*, *106*, 28,089–28,095.

Perkins, M., W. Nash, F. Brown, and R. Fleck (1995), Fallout tuffs of Trapper Creek, Idaho: A record of Miocene explosive volcanism in the Snake River Plain volcanic province, *Geol. Soc. Am. Bull.*, *107*, 1484–1506.

Petit, J. R., et al. (1999), Climate and atmospheric history of the past 42,0000 years from the Vostok ice core, *Antarctica, Nature*, *399*, 429–436.

Prata, A. J., W. I. Rose, S. Self, and D. M. O'Brien (2003), Global, long-term sulphur dioxide measurements from TOVS data: A new tool for studying explosive volcanism and climate, in *Volcanism and the Earth's Atmosphere*, *Geophys. Monogr. Ser.*, vol. 139, edited by A. Robock and C. Oppenheimer, pp. 75–92, AGU, Washington, D. C.

Rampino, M. R., and S. Self (1982), Historic eruptions of Tambora, 1815. Krakatau, 1883. and Agung, 1963. their stratospheric aerosols, and climatic impact, *Quat. Res.*, *18*, 127–143.

Rampino, M. R., and S. Self (1984), Sulfur-rich volcanic eruptions and stratospheric aerosols, *Nature*, *310*, 677–679.

Rampino, M. R., S. Self, and R. W. Fairbridge (1979), Can rapid climatic change cause volcanic eruptions?, *Science*, *206*, 826–829.

Rankin, A. M., and E. W. Wolff (2003), A year-long record of size-segregated aerosol composition at Halley, Antarctica, *J. Geophys. Res.*, *108*(D24), 4775, doi:10.1029/2003JD003993.

Robock, A. (2000), Volcanic eruptions and climate, *Rev. Geophys.*, *38*, 191–219.

Robock, A., and M. P. Free (1995), Ice cores as an index of global volcanism from 1850 to the present, *J. Geophys. Res.*, *100*, 11,549–11,568.

Rose, W. I., and C. A. Chesner (1987), Dispersal of ash in the great Toba eruption, 75,000 years B.P., *Geology*, *15*, 913–917.

Rosi, M., P. Landi, M. Polacci, A. Di Muro, and D. Zandomeneghi (2004), Role of conduit shear on ascent of the crystal-rich magma feeding the 800-year-B.P. Plinian eruption of Quilotoa volcano (Ecuador), *Bull. Volcanol.*, *66*, 307–321.

Rothlisberger, R., R. Mulvaney, E. W. Wolff, M. A. Hutterli, M. Bigler, M. de Angelis, M. E. Hansson, J. P. Steffensen, and R. Udisti (2003), Limited dechlorination of sea-salt aerosols during the last glacial period: Evidence from the European Project for Ice Coring in Antarctica (EPICA) Dome C ice core, *J. Geophys. Res.*, *108*(D16), 4526, doi:10.1029/2003JD003604.

Self, S., and R. S. J. Sparks (1981), *Tephra Studies*, 481 pp., Springer, New York.

Self, S., M. Rampino, and J. J. Barbera (1981), The possible effects of large 19th and 20th century volcanic eruptions on zonal and hemispheric surface temperatures, *J. Volcanol. Geotherm. Res.*, *11*, 41–60.

Simkin, T., and L. Siebert (1994), *Volcanoes of the World: A Regional Directory, Gazetteer, and Chronology of Volcanism During the Last 10,000 Years*, 2nd ed., 349 pp., Geoscience, Tucson, Ariz.

Simkin, T., and L. Siebert (2002–2005), Volcanoes of the World: An Illustrated Catalog of Holocene Volcanoes and Their Eruptions *Digital Inf. Ser. GVP-3*, Global Volcan. Program, Smithsonian Inst., Washington, D. C. (Available at http://www.volcano.si.edu/world/)

Smellie, J. L. (1999), The upper Cenozoic tephra record in the south polar region: A review, distal tephrochronology, tephrology and volcano-related atmospheric effects, *Global Planet. Change*, *21*, 51–70.

Stenni, B., M. Proposito, R. Gragnani, O. Flora, J. Jouzel, S. Falourd, and M. Frezzotti (2002), Eight centuries of volcanic signal and climate change at Talos Dome (East Antarctica), *J. Geophys. Res.*, *107*(D9), 4076, doi:10.1029/2000JD000317.

Stuiver, M., P. J. Reimer, E. Bard, J. W. Beck, G. S. Burr, K. A. Hughen, B. Kromer, F. G. McCormac, J. van der Plicht, and M. Spurk (1998), INTCAL98 Radiocarbon age calibration 24,000-0 cal B.P., *Radiocarbon*, *40*, 1041–1083.

Taylor, K. C., and R. B. Alley (2004), Two-dimensional electrical stratigraphy of the Siple Dome (Antarctica) ice core, *J. Glaciol.*, *50*(169), 231–235.

Taylor, K. C., C. U. Hammer, R. B. Alley, H. B. Clausen, D. Dahl-Jensen, A. J. Gow, N. S. Fundestrup, J. Kipfstuhl, J. C. Moore, and E. D. Waddington (1993), Electrical conductivity measurements from the GISP2 and GRIP Greenland ice cores, *Nature*, *366*, 549–552.

Taylor, K. C., et al. (2004), Dating the Siple Dome (Antarctica) ice core by manual and computer interpretation of annual layering, *J. Glaciol.*, *50*(170), 453–461.

Thorarinsson, S. (1944), Tephrochronological studies in Iceland, *Geograf. Ann.*, *26*, 1–217.

Tilling, R. I., M. Rubin, H. Sigurdsson, S. Carey, W. A. Duffield, and W. I. Rose (1984), Holocene eruptive activity of El Chichón volcano, Chiapas, Mexico, *Science*, *224*, 747–749.

Udisti, R., S. Becagli, E. Castellano, R. Mulvaney, J. Schwander, S. Torcini, and E. Wolff (2000), Holocene electrical and chemical measurements from the EPICA-Dome C ice core, *Ann. Glaciol.*, *30*, 20–26.

von Storch, H., and F. W. Zwiers (2001), *Statistical Analysis in Climate Research*, 484 pp., Cambridge Univ. Press, New York.

Wagenbach, D. (1996), Coastal Antarctica: Atmospheric chemical composition and atmospheric transport, in *Chemical Exchange Between the Atmosphere and Polar Snow*, *NATO ASI Ser., Ser. I*, vol. 43, edited by E. W. Wolf and R. C. Bales, pp. 173–199, Springer, New York.

Wilch, T. I., W. C. McIntosh, and N. W. Dunbar (1999), Late Quaternary volcanic activity in Marie Byrd Land: Potential $^{40}Ar/^{39}Ar$ dated time horizons in West Antarctic ice and marine cores, *Geol. Soc. Am. Bull.*, *111*, 1563–1580.

Wolff, E. W., J. C. Moore, H. B. Clausen, C. U. Hammer, J. Kipfstuhl, and K. Fuhrer (1995), Long-term changes in the acid and salt concentrations of the Greenland Ice Core Project ice core from electrical stratigraphy, *J. Geophys. Res.*, *100*, 16,249–16,263.

Worner, G., L. Viereck, J. Hertogen, and H. Niephaus (1989), The Mt. Melbourne Volcanic Field (Victoria Land, Antarctica), II. Geochemistry and magma genesis, in *GANOVEX IV*, edited by D. Damaske and H. J. Durbaum, pp. 395–434, Herausgegeben von der Bundesanst. fur Geowiss. und Rohstoffe, Hanover, Germany.

Wright, A. C., and P. R. Kyle (1990), Royal Society Range, in *Volcanoes of the Antarctic Plate and Southern Oceans*, *Antarct. Res. Ser.*, vol. 48, edited by W. E. LeMasurier, and J. W. Thomson, pp. 131–133, AGU, Washington, D. C.

Zdanowicz, C. M., G. A. Zielinski, and S. Germani (1999), Mount Mazama eruption: Calendrical age verified and atmospheric impact assessed, *Geology*, *27*(7), 621–624.

Zielinski, G. A. (1995), Stratospheric loading and optical depth estimates of explosive volcanism over the last 2100 years derived from the Greenland Ice Sheet Project 2 ice core, *J. Geophys. Res.*, *100*, 20,937–20,955.

Zielinski, G. A. (2000), Use of paleo-records in determining variability within the volcanism-climate system, *Quat. Sci. Rev.*, *19*, 417–438.

Zielinski, G. A., and M. S. Germani (1998), New ice core evidence challenges the 1620s BC age for the Santorini (Minoan) eruption, *J. Archaeol. Sci.*, *25*, 279–289.

Zielinski, G. A., P. A. Mayewski, L. D. Meeker, S. Whitlow, M. S. Twickler, M. Morrison, D. A. Meese, A. J. Gow, and R. B. Alley (1994), Record of volcanism since 7000 B.C. from the GISP 2 Greenland ice core and implications for the volcano-climate system, *Science*, *264*, 948–952.

Zielinski, G. A., M. S. Germani, G. Larsen, M. G. L. Baillie, S. Whitlow, M. S. Twickler, and K. Taylor (1995), Evidence of the Eldgia (Iceland) eruption in the GISP2 Greenland ice core: Relationship to eruption processes and climate conditions in the tenth century, *Holocene*, *5*, 129–140.

Zielinski, G. A., P. A. Mayewski, L. D. Meeker, S. Whitlow, M. S. Twickler, and K. Taylor (1996a), Potential atmospheric impact of the Toba mega-eruption 71,000 years ago, *Geophys. Res. Lett.*, *23*(8), 837–840.

Zielinski, G. A., P. A. Mayewski, L. D. Meeker, S. Whitlow, and M. S. Twickler (1996b), A 11,0000-yr record of explosive volcanism from the GISP2 (Greenland) ice core, *Quat. Res.*, *45*, 109–118.

Zielinski, G. A., J. E. Dibb, Q. Yang, P. A. Mayewski, S. Whitlow, M. S. Twickler, and M. S. Germani (1997a), Assessment of the record of the 1982 El Chichón eruption as preserved in Greenland snow, *J. Geophys. Res.*, *102*, 30,031–30,045.

Zielinski, G. A., P. A. Mayewski, L. D. Meeker, K. Grönvold, M. S. Germani, S. Whitlow, M. S. Twickler, and K. Taylor (1997b), Volcanic aerosol records and tephrochronology of the Summit, Greenland, ice cores, *J. Geophys. Res.*, *102*, 26,625–26,640.

N. W. Dunbar, New Mexico Bureau of Geology and Mineral Resources, New Mexico Institute of Mining and Technology, 801 Leroy Place, Socorro, NM 87801, USA. (nelia@nmt.edu)

A. V. Kurbatov, P. A. Mayewski, E. A. Meyerson, S. B. Sneed, and G. A. Zielinski, Climate Change Institute, 303 Bryand Global Sciences Center, University of Maine, Orono, ME 04469, USA. (akurbatov@maine.edu; paul.mayewski@maine.edu; eric.meyerson@maine.edu; sharon.sneed@maine.edu; gzielinski@maine.edu)

K. C. Taylor, Desert Research Institute, University of Nevada, 2215 Raggio Parkway, Reno, NV 89511, USA. (kendrick@dri.edu)